

Document downloaded from:

<http://hdl.handle.net/10251/83444>

This paper must be cited as:

Gómez Jiménez, MD.; Ventimilla-Llora, D.; Sacristán Tarrazó, R.; Perez Amador, MA. (2016). Gibberellins Regulate Ovule Integument Development by Interfering with the Transcription Factor ATS. *Plant Physiology*. 172(4):2403-2415. doi:10.1104/pp.16.01231.



The final publication is available at

<http://doi.org/10.1104/pp.16.01231>

Copyright American Society of Plant Biologists

Additional Information

1 **Short title:**

2 Gibberellins and ATS in ovule development

3

4 **Corresponding author:**

5 Miguel A Perez-Amador

6 Instituto de Biología Molecular y Celular de Plantas (IBMCP), Universidad Politécnica
7 de Valencia-Consejo Superior de Investigaciones Científicas (CSIC). Ingeniero Fausto
8 Elio s/n, 46022 Valencia, Spain. mpereza@ibmcp.upv.es, +34-963877723

9

10 **Title:**

11 **Gibberellins regulate ovule integument development by interfering with the**
12 **transcription factor ATS**

13

14 **Author names and affiliations**

15 MD Gomez, Ventimilla D¹, Sacristan R, Perez-Amador MA*

16

17 **Address:**

18 Instituto de Biología Molecular y Celular de Plantas (IBMCP), Universidad Politécnica
19 de Valencia-Consejo Superior de Investigaciones Científicas (CSIC). Ingeniero Fausto
20 Elio s/n, 46022 Valencia, Spain

21

22 **One sentence summary**

23 Gibberellins negatively regulate integument growth in ovules through destabilization of
24 the DELLA-ATS protein complex

25

26 **Author contribution**

27 MD.G. performed most of the experiments; D.V. carried out protein-protein binding
28 assays; R.S. analyzed DELLA mutants; MA.P-A. performed mutant seed analysis;
29 MD.G. and MA.P-A. conceived the project, analyzed and interpreted data, and wrote
30 the article with contributions by all the authors.

31

32

33

34 **Funding:**

35 This work has been supported by grants BIO2011-26302 and BIO2014-55946 from the
36 Spanish Ministry of Science and Innovation and the Spanish Ministry of Economy and
37 Competitiveness, respectively, and ACOMP/2013/048, and ACOMP/2014/106 from the
38 Generalitat Valenciana for MA.P-A. R.S. received a PhD fellowship from the Spanish
39 Ministry of Science and Innovation.

40

41 **Present address:**

42 ¹, Instituto Valenciano de Investigaciones Agrarias (IVIA), Carretera Moncada-
43 Naquera, Km. 4.5, 46113 Moncada, Valencia, Spain

44

45 **Corresponding autor e-mail:**

46 mpereza@ibmcp.upv.es

47

48 **ABSTRACT**

49

50 Gibberellins (GAs) are plant hormones that regulate most plant life cycle aspects,
51 including flowering and fruit development. Here we demonstrate the implication of
52 GAs in ovule development. DELLA proteins, negative GA response regulators, act as
53 positive factors for ovule integument development in a mechanism that involves
54 transcription factor ATS. The seeds of the *della global* mutant, a complete loss-of
55 function of DELLA, and the *ats-1* mutant are remarkably similar, with a round shape, a
56 disorganized testa, and viviparism. These defects are the result of an alteration in
57 integuments that fail to fully develop and are shorter than in WT plants. *ats-1* also
58 shows some GA-related phenotypes, e.g. higher germination rates and early flowering.
59 In fact, *ats-1* has elevated GA levels due to the activation of GA biosynthesis genes,
60 which indicates that ATS inhibits GA biosynthesis. Moreover, DELLAs and ATS
61 proteins interact, which suggests the formation of a transcriptional complex that
62 regulates the expression of genes involved in integument growth. Therefore, the
63 repression of GA biosynthesis by ATS would result in the stabilization of DELLAs to
64 ensure correct ATS-DELLA complex formation. The requirement of both activities to
65 coordinate proper ovule development strongly argues that the ATS-DELLA complex
66 acts as a key molecular factor. This work provides the first evidence for a role of GAs in
67 ovule and seed development.

68

69 **INTRODUCTION**

70

71 Gibberellins (GAs) are plant tetracyclic diterpenoids that play a major role in diverse
72 key developmental processes throughout the plant life cycle, including seed
73 germination, stem and root elongation, flowering, and fruit development (Sun, 2010;
74 Gupta and Chakrabarty, 2013). The master regulator in GA signaling is the DELLA
75 protein, a subfamily of the plant-specific GRAS family of transcriptional regulators
76 (Sun, 2010). Bioactive GAs are perceived by receptor GID1s to allow GA-GID1-
77 DELLA complex formation, which results in structural changes in the DELLA protein
78 that trigger recognition and binding with F-box proteins, polyubiquitination and
79 subsequent degradation by the 26S proteasome (Sun, 2011). Therefore, while DELLA
80 proteins act as plant growth repressors, GAs promote growth and development by the
81 rapid degradation of DELLA proteins. Accordingly, lack of DELLA activity in different
82 mutants of *Arabidopsis* (Cheng et al., 2004; Feng et al., 2008), tomato (Jasinski et al.,
83 2008; Bassel et al., 2008), or rice (Ikeda et al., 2001) results in a constitutive GA
84 response. On the contrary, the mutant alleles of the DELLAs that lack the amino
85 domain DELLA, like *gai-1* (Peng et al., 1997) or pRGA:*GFP-rgaA17* (Dill et al., 2001)
86 of *Arabidopsis*, and *Slr1-d* in rice (Asano et al., 2009), encode proteins that cannot be
87 degraded, which results in constitutive DELLA activity and GA response blockage.
88 Unlike most analyzed plant species that encode a single DELLA protein, the
89 *Arabidopsis* genome encodes five DELLAs: GA-INSENSITIVE (GAI), REPRESSOR
90 OF *gal-3* (RGA), RGA-LIKE1 (RGL1), RGL2, and RGL3. Each one performs distinct,
91 but also overlapping, functions in repressing GA responses (Sun, 2011).

92 DELLA proteins function as central nodes that integrate hormonal and
93 environmental cues to modulate transcriptional patterns, which finally regulate growth
94 and development (Daviere and Achard, 2016). DELLAs lack a canonical DNA binding
95 domain, and thus mediate the transcriptional regulation of the target genes involved in
96 the GA response throughout the direct physical interaction with transcription factors
97 (TFs) and other regulatory proteins (Vera-Sirera et al., 2015; Daviere and Achard,
98 2016). DELLA-TF binding can be divided into two major mechanisms. DELLAs can
99 bind to either TFs or other transcriptional regulators to block their function, or bind to
100 TF linked to the promoter of target the genes, modulating their transcriptional activity
101 (Daviere and Achard, 2016). The list of potential DELLA interactors has rapidly
102 increased and provided direct evidence for not only the mechanism of crosstalk between

103 GAs and other hormones, but also for environmental clues to modulate adequate plant
104 growth and response to environmental conditions (Marin-de la Rosa et al., 2014, 2015;
105 Daviere and Achard, 2016).

106 GAs and DELLAs are key players during fruit development (Vivian-Smith and
107 Koltunow, 1999; Dorcey et al., 2009; Fuentes et al., 2012). Under normal conditions,
108 the unfertilized pistils do not develop into fruits due to low GA levels. Upon
109 fertilization, GA metabolism is activated which, in turn, triggers GA signaling and fruit
110 development (Hu et al., 2008; Rieu et al., 2008; Dorcey et al., 2009). DELLAs are
111 negative factors in early fruit development steps. In *Arabidopsis*, loss of function of at
112 least four out of the five DELLAs promotes facultative parthenocarpic fruit growth
113 (Dorcey et al., 2009; Fuentes et al., 2012). DELLAs also control other aspects during
114 fruit development, such as endocarp degradation and lignification, which are
115 respectively delayed or advanced in the loss of function mutant of the GA receptors
116 *GID1* or in the *della global* mutant, (lacking all five DELLAs; thereafter known as
117 *global* mutant) (Dorcey et al., 2009; Gallego-Giraldo et al., 2014).

118 Despite all these data, very little is known about the role of GAs during early
119 pistil ontogeny, except for valve margin differentiation (Arnaud et al., 2010).
120 *ALCATRAZ* (*ALC*) is a bHLH protein involved in the formation of the dehiscence
121 zone in the valve margin, required for fruit shattering and seed dispersal. DELLAs
122 block *ALC* activity in the specification of the separation cell layer in the dehiscence
123 zone by means of direct DELLA-*ALC* protein binding.

124 No previous evidences have implicated the GAs in ovule initiation and
125 formation, a key developmental process that occurs during early pistil ontogeny. Ovules
126 emerge from the placental tissue as finger-like primordia at stage 8 of flower
127 development (Smyth et al., 1990; Modrusan et al., 1994). Later, three different regions
128 can be distinguished along the proximal-distal axis: the funiculus, which attaches the
129 ovule to the placenta, the chalaza, and the nucellus, which encloses the megaspore
130 mother cell. Integuments develop asymmetrically from the chalaza surrounding the
131 nucellus. The outer integument totally overgrows the inner integument in the mature
132 ovule. Upon fertilization, cells in both the outer and the inner integument undergo a
133 transformation process, which gives rise to the testa or seed coat (Western et al., 2001;
134 Haughn and Chaudhury, 2005). Therefore, the structure and morphology of the mature
135 testa depend on the correct initiation and growth of integuments. Consequently,

136 regulation of integument development can have vast effects on the final testa structure
137 and composition.

138 Numerous genes involved in integument patterning and growth have been
139 identified (Sieber et al., 2004; Battaglia et al., 2009; Kelley and Gasser, 2009). One
140 such gene is *ABERRANT TESTA SHAPE* (*ATS*, *At5g42630*) (McAbee et al., 2006),
141 which encodes a KANADI (KAN) TF, previously named KAN4. *ATS* provides
142 boundary maintenance and promotes the laminar growth of the inner ovule integument.
143 Loss of the *ATS* function in the *ats-1* mutant leads to the fusion of the inner and outer
144 integuments that grow as a unit to produce a single fused structure. As a result of this
145 fusion, *ats-1* seeds are abnormally rounded and variable in size (Leon-Kloosterziel et
146 al., 1994; McAbee et al., 2006).

147 Here we describe the implication of GAs as negative factors in integument
148 growth during ovule ontogeny, and how DELLAs are required for correct integuments
149 formation. DELLA activity would be mediated by its direct interaction with the
150 KANADI TF *ATS/KAN4*. Our data suggest that the *ATS-DELLA* complex is a key
151 molecular factor for regulating the transcription of the genes involved in ovule
152 integument growth. The positive role of DELLAs and the detrimental effect of
153 constitutive GA signaling on ovule development contrast with the traditional view of
154 the DELLAs as negative growth regulators. This is the first evidence for the implication
155 of DELLAs in the development of ovules. We propose a molecular model of the
156 function of DELLAs and *ATS* during integument grow.

157

158

159

160 RESULTS

161

162 DELLAs participate in seed formation

163 Constitutive GA signaling in *Arabidopsis* multiple DELLA loss-of-function
164 mutants gives rise to fruits with fewer seeds and shorter in length than those in *Ler*
165 (WT) plants (Cao et al., 2005; Dorcey et al., 2009). To gain a better picture of the role
166 of GAs in seed development, we thoroughly analyzed the number and morphology of
167 the seeds in the *global* mutant (the quintuple *gaiT6 rgaT2 rgl1-1 rgl2-1 rgl3-1* mutant).
168 All the assays were carried out in fruits from emasculated flowers pollinated with WT
169 pollen to ensure that only maternal effects were tested. The seed number of the *global*
170 mutant lowered by 60%, while fruit length shortened only by 30%, which resulted in
171 lower seed density per fruit (Fig. 1, A and B). In many species, including *Arabidopsis*,
172 fruit size correlates with seed number (Cox and Swain, 2006), which suggests that the
173 facultative parthenocarpy of the *global* mutant, due to constitutive GA signaling, may
174 account for the further elongation of these fruits and lower seed density. While mature
175 fruits of WT plants had seed-filled siliques, the fruits of the *global* mutant had many
176 aborted seeds (Fig. 1C). More importantly, the *global* mutant mature seeds were
177 irregularly round in shape and smaller than the WT seeds (Fig. 1, C-E). The *della*
178 *quadruple* mutant of *GAI*, *RGA*, *RGL1* and *RGL2* showed a similar phenotype (shorter
179 fruits, fewer and rounded seeds, and parthenocarpy), which indicates that the function of
180 these four DELLA proteins were required for proper seed development, and that *RGL3*
181 was not involved (Supplemental Fig. S1; Dorcey et al., 2009). In contrast, any of the
182 four triple *della* mutants of *GAI*, *RGA*, *RGL1*, and *RGL2* showed parthenocarpy or
183 defects in seed morphology, which would suggest that both processes share a common
184 genetic basis (Supplemental Fig. S1).

185 The testa of the *global* mutant seeds was defective (Fig. 1D). The epidermal
186 cells in the testa are characterized by polygonal structures with a central elevation or
187 columella. In contrast, the epidermal cells of *global* mutant seeds clearly lacked this
188 structure and were less regular in shape. These modifications may diminish the
189 mechanical restriction to embryo growth and collaborate with GA constitutive signaling
190 in the viviparism occurrence (germination inside the silique) in *global* mutant seeds
191 (Fig. 1E). Alteration in the testa and seed shape of the *global* mutant did not interfere
192 with seed viability, which indicates that embryo development is not altered (see below
193 for seed germination assays). All defects in the *global* mutant seeds are exclusively

Figure 1. Gomez et al.

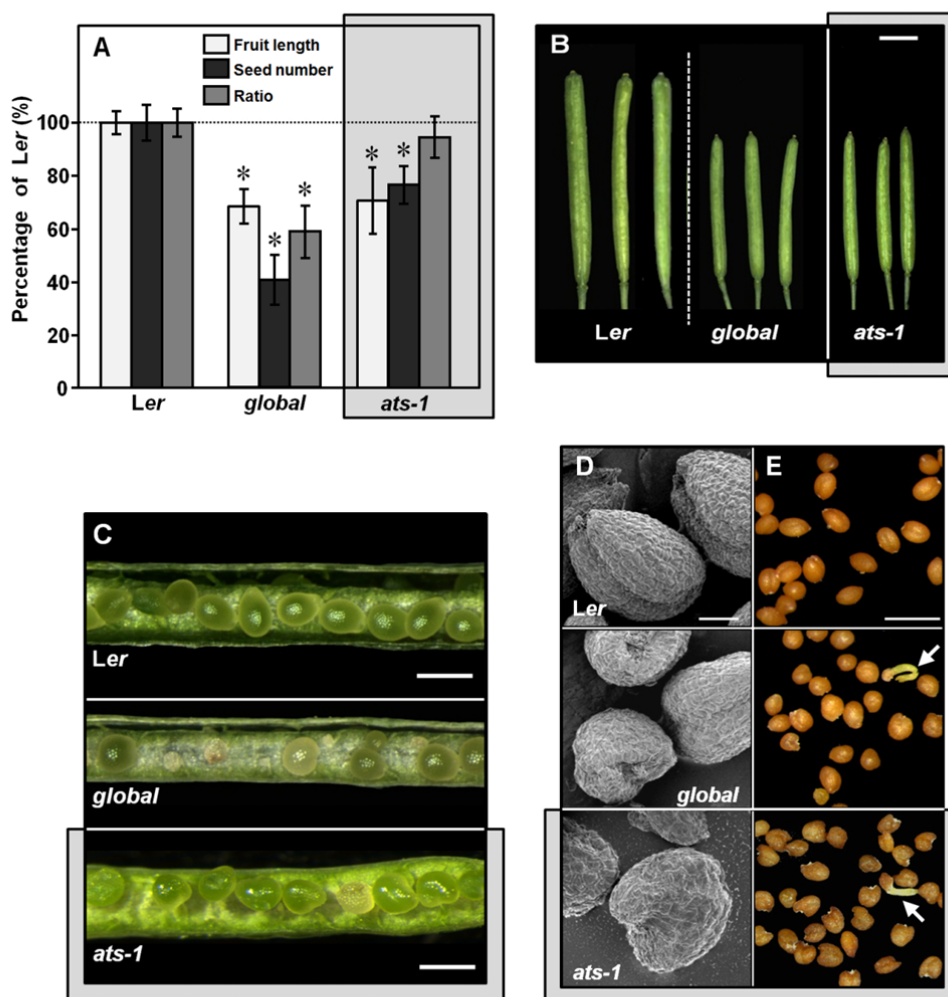


Figure 1. Constitutive GA signaling in the *della global* mutant causes seed defects and reduced fertility, similarly to *ats-1*.

A, Silique length, seed number, and length/width ratio in fruits of *Ler* and the *global* and *ats-1* mutants at 12 days-post-anthesis (dpa). Data are the mean and standard error (SE) of three independent experiments, each one from at least 50 fruits. The significant differences (Student's t-test analysis) between *Ler* and mutants are marked with asterisks (* p-value < 0.01). **B-C**, Images of whole (**B**) and open (**C**) 8-dpa fruits of *Ler*, and the *global* and *ats-1* mutants. **D-E**, Images of mature seeds of *Ler*, and the *global* and *ats-1* mutants, taken by SEM (**D**) or stereomicroscope (**E**). The white arrow marks the viviparous seeds of the *ats-1* and mutants. All the images in each category have the same magnification. Scale bars represent 2 mm in **B**, 500 μ m in **C** and **E**, and 100 μ m in **D**.

194 attributable to maternal tissue as all the assays were carried out in emasculated flowers
 195 that were hand-pollinated with WT pollen.

196 DELLA activity during seed formation was also tested using the gain-of-
 197 function *gai-1* mutant. The *gai-1* seeds showed apparently unaltered seed morphology,
 198 but were 25% larger than those of the WT, due to an increase along the major axis (Fig.
 199 2, A-C), in contrast to the *global* seeds that were 25% shorter in length than WT seeds

Figure 2. Gomez et al.

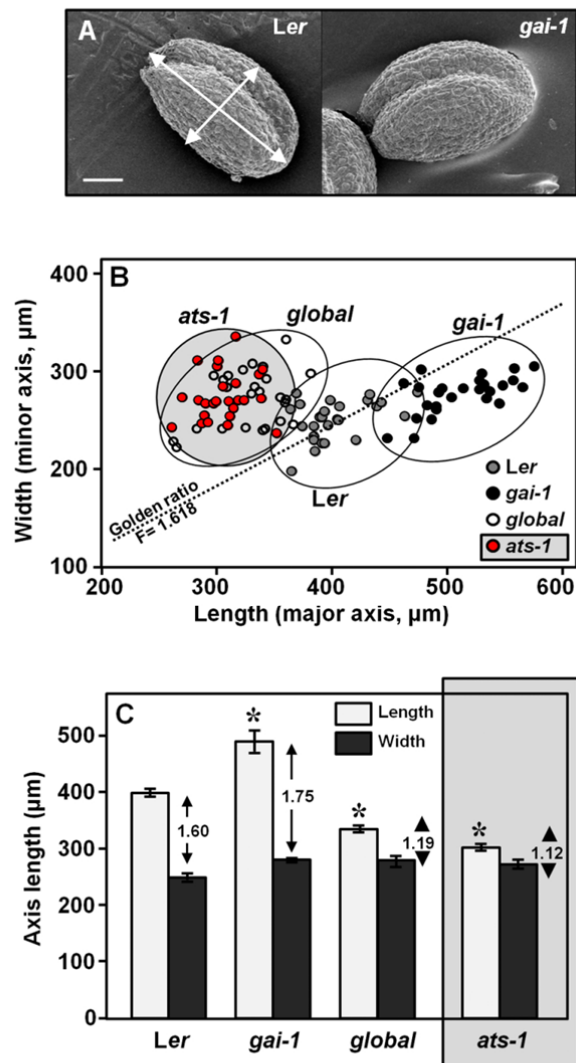


Figure 2. DELLAs and ATS regulate seed size and shape.

A, SEM images of mature seeds of *Ler* and the *gai-1* mutant. Length and width (major and minor axis, respectively) are marked with white arrows in *Ler* seed. **B,** Size distribution of mature seeds of *Ler* and the *gai-1*, *global* and *ats-1* mutants, represented as length (major axis) and width (minor axis). Golden ratio is represented by a line at the 1,618 ratio. **C,** Seed length and width of *Ler* and the *gai-1*, *global*, and *ats-1* mutants. Data are the mean \pm SE of three biological replicas, each one from 25-30 seeds. Significant differences (Student's *t*-test analysis) between *Ler* and mutants are marked with asterisks (* *p*-value < 0.01). The ratio between seed length and width is indicated.

200 (Fig. 2, B and C). No significant defects were detected in the width of seeds from the
 201 *global* or *gai-1* mutants. It has been reported that length and width of *Arabidopsis* WT
 202 seeds follow the Golden ratio (Cervantes et al., 2010), also known as the divine
 203 proportion, a mathematical constant ($\Phi=1.618$) frequently found in many biological-
 204 based geometries. The length/width ratio of the WT seeds was 1.60, which came very

205 close to the Golden ratio. In contrast, the ratio in the *gai-1* and *global* mutants was 1.75
206 and 1.19, respectively, which reflects the enlarged and shorter seed shape caused by the
207 gain- and loss-of function of the DELLA functions. These results indicate that DELLA
208 activity is required for proper seed growth and development, mainly on the
209 proximal/distal axis.

210

211 **The *della global* mutant has defects in integument development**

212 The testa is differentiated from ovule integuments (Beeckman et al., 2000).
213 Therefore, the majority of mutants with structural defects in the testa are affected in
214 integument development. Figure 3 shows ovule and seed development in the *global*
215 mutant and WT. At early ovule development, no clear distinction was noticed (Fig. 3A),
216 but altered growth of integuments was observed at stage 3-II in the *global* mutant
217 (Schneitz et al., 1995). Integuments were shorter, with no clear distinction among their
218 different cell layers. As a consequence, at anthesis, only two cell layers in each
219 integument were formed, and the outer integument did not cover the nucellus,
220 displaying an altered shape (Fig. 3C). In contrast to the *global* mutant, a WT ovule at
221 anthesis is formed by two layers of cells in the outer integument and three layers of the
222 inner integument; the outer integument has overgrown the shorter inner integument
223 around the embryo sac. Developing seeds of the *global* mutant clearly showed unusual
224 testa development, with three-four cell layers, unlike the five well-defined cell layers of
225 a WT seed, with full or partial endothelium layer, depending on the severity of
226 phenotype (Fig. 3, D and E). Therefore, the altered ovule development of the *global*
227 mutant is the most possible cause of the abnormal seed morphology.

228

229 **The ovule and seed phenotypes of the *global* mutant resemble those of the *ats-1* 230 mutant**

231 Similar alterations in mature ovules to those in the *global* mutant were observed
232 in the null *aberrant testa shape-1 (ats-1)* mutant (Leon-Kloosterziel et al., 1994).
233 *ATS/KAN4 (At5g42630)*, encodes one of the four KANADI gene family members
234 (Hawker and Bowman, 2004), a subset of the GARP (from GOLDEN2, ARR-B Class,
235 Par1 proteins) family of putative TF genes which play roles in leaf polarity and
236 expansion, and also in ovule development (Eshed et al., 2001; McAbee et al., 2006).

237 To facilitate comparisons, the data from *ats-1* are shown along with data from
238 the *global* mutant in Figures 1, Figure 2 and Figure 3. The siliques of *ats-1* are shorter

Figure 3. Gomez et al.

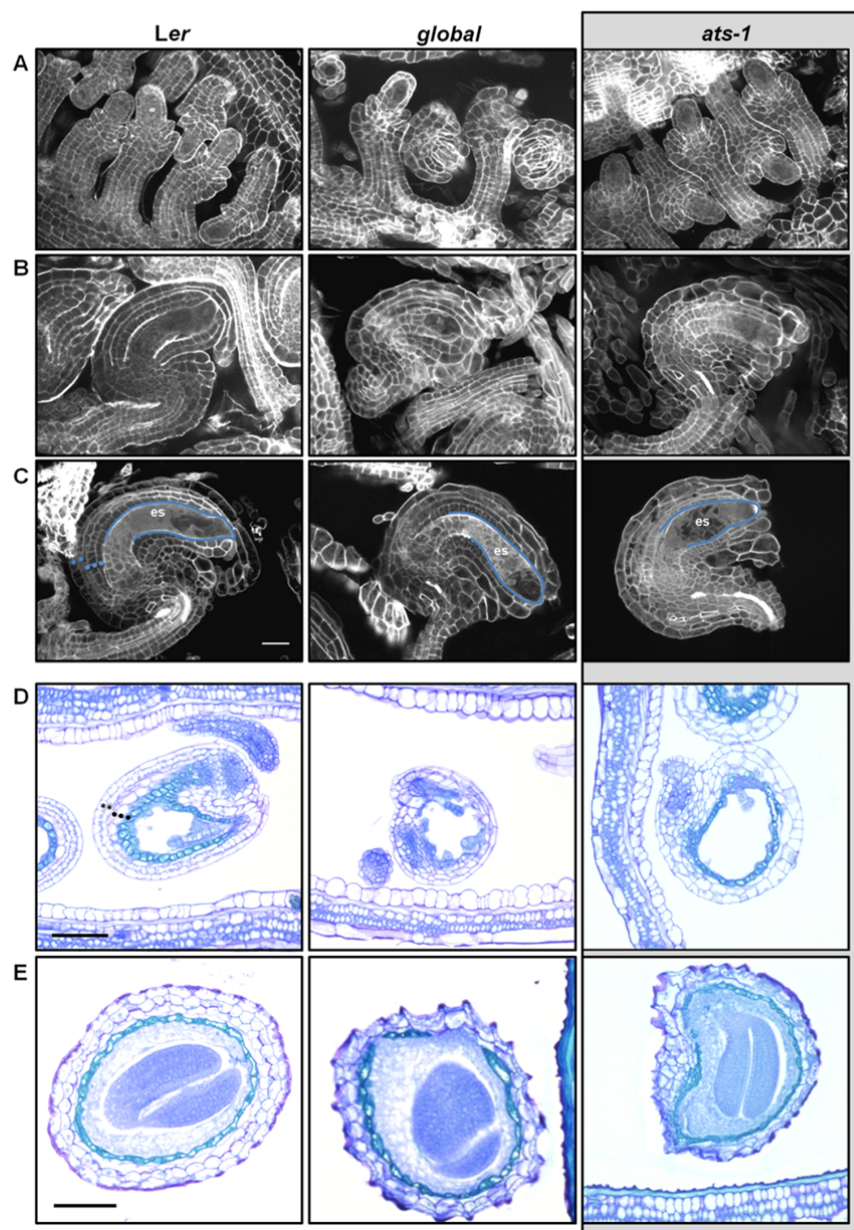


Figure 3. DELLAs and ATS regulate ovule integument development.

A-B, Images of *Ler*, *global* and *ats-1* ovules at stage 2-III (A) and 3-II (B) (Schneitz et al., 1995).

C, Images of ovules at anthesis. The shape of the embryo sac (es) is marked by blue lines.

D-E, Transversal section of fertilized ovules at 3 dpa (D) or 7 dpa (E).

The outer and inner integument layers of WT in C and D are indicated with asterisks

and dots, respectively. Scale bars represent 50 μm in A, B and C and 100 μm in D and E.

239 and contain fewer seeds than WT, but unlike the *global* mutant, *ats-1* showed a
 240 proportional reduction of seed number and silique length, resulting in a ratio similar to
 241 WT (Fig. 1, A and B) as *ats-1* does not display parthenocarpy (Vivian-Smith et al.,
 242 2001). The *ats-1* siliques also contained aborted seeds, with defects in the testa and
 243 viviparism (Fig. 1, C-E), and were smaller, globular in shape, and had a length/width

244 ratio of 1.12, (Fig. 2, B and C). Moreover, the ovules of *ats-1* at anthesis resembled to
245 those of the *global* mutant, with short integuments that did not cover the embryo sac at
246 the micropyle and fewer integument layers (Fig. 3C). Unlike *global* mutant, *ats-1* outer
247 and inner integuments were fused, with no separation space between them from early
248 developmental stages (Fig. 3A) (Leon-Kloosterziel et al., 1994; McAbee et al., 2006).
249 In contrast, at stage 3-II, integuments of *ats-1* arrested growth and did not extend
250 beyond the embryo sac, similarly to the *global* mutant (Fig. 3B). Defects in testa during
251 seed development of both *global* and *ats-1* were also very similar (Fig. 3, D and E),
252 Although both *global* and *ats-1* mutants showed different ovule integument
253 development in early stages, we pursued the study of ATS role in the GA regulation of
254 ovule growth based on two key observations: ATS was a potential binding protein to the
255 DELLAs (Marin-de la Rosa et al., 2015) and *ats-1* displayed typical GA-related
256 phenotypes.

257

258 ***ats-1* displays GA signaling phenotypes**

259 We have shown that the ovule and seed defects of *ats-1* closely resembled those
260 of the *global* mutant. Interestingly, *ats-1* also showed GA-related phenotypes (Fig. 4).
261 The *ats-1* plants had similar alterations in germination and flowering to those observed
262 in plants with a constitutive GA signaling response. GAs play a central role in
263 germination by promoting testa breakage and facilitating radicle protrusion. Loss of
264 DELLA activity in the *global* mutant plants led to both light- and GA-independent seed
265 germination, with RGL2 being the predominant repressor of seed germination (Lee et
266 al., 2002; Cao et al., 2005). The *ats-1* mutant seeds showed higher germination rate
267 compared to those of the WT, but lower than those of the *global* and *rgl2-1* mutants
268 (Fig. 4A). However, the *ats-1* seeds germinated at a similar rate to the null *rgl2-1*
269 mutant in the presence of the GA inhibitor paclobutrazol (PCB). Lack of ATS function
270 overcame the seed germination inhibition produced by the stabilized DELLA proteins
271 by PCB, which indicates that ATS plays a role as a repressor of germination. Finally,
272 the alterations in ovule and seed morphology observed in the *ats-1* and *global* mutants
273 did not affect embryo viability as the germination rates were high, especially in PCB.

274 GAs regulate flowering time and stem elongation, especially under short days
275 (Galvao et al., 2012; Porri et al., 2012). Coinciding with a possible GA-related
276 phenotype caused by the loss-of-function of ATS, the flowering time of the *ats-1* plants
277 advanced particularly in short days (Fig. 4B). The *ats-1* mutant plants also flowered

Figure 4. Gomez et al.

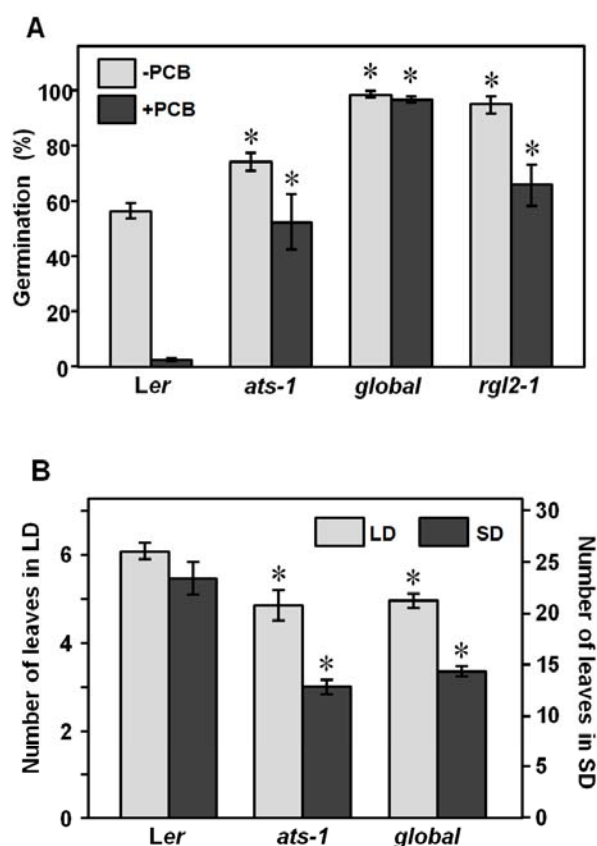


Figure 4. *ats-1* shows higher seed germination and early flowering.

A, Germination rate of *Ler* and the *ats-1*, *global*, and *rgl2-1* mutants. Germination was scored at 3 days in the absence (-PCB) or presence of 1 μ M of PCB (+PCB). **B**, Flowering time of *Ler* and the *ats-1* and *global* mutants. Flowering was scored as the number of leaves in plants grown in long (LD) and short (SD) days. Significant differences (Student's *t*-test analysis) between *Ler* and mutants are indicated by an asterisk (*, *p*-value < 0.01). Data are the mean \pm SE of three biological replicas, each one from 80-100 seeds in A and 30-40 plants in B.

278 slightly earlier than the WT under long days. Early flowering of *ats-1* was very similar
279 to that of the *global* mutant (Fig. 4B). Taken together our data suggest that ATS and
280 DELLA may participate in germination and flowering, and also in ovule/seed
281 formation, through a common molecular mechanism. These analysis uncovered new
282 functions of ATS, beyond ovule and seed development reported previously.
283 Interestingly, there is a discrepancy between the known *ATS* expression pattern and the
284 spatial distribution of phenotypes, which would be further explained by possible

285 indirect effects, non cell autonomy of ATS function, or the lack of a comprehensive
286 determination of the *ATS* expression.

287

288 **ATS inhibits GA biosynthesis**

289 We hypothesized that an increase in GA content in *ats-1* could be the reason for
290 the GA-related phenotypes described above. Direct quantification of the GA forms that
291 belonged to the non-13-hydroxylated pathway, which contributes mainly to the
292 biosynthesis of the bioactive GA₄, supported a role of ATS in inhibiting GA
293 biosynthesis (Fig. 5A). Levels of GA₄ increased 3-fold in *ats-1* compared with the WT,
294 while levels of intermediates GA₁₂ and GA₂₄, and the inactivated form GA₅₁, were also
295 significantly increased. Furthermore, expression of GA biosynthesis genes *GA20ox2*,
296 *GA3ox1*, and *GA3ox2*, but not *GA20ox1*, was up-regulated in *ats-1* (Supplemental Fig.
297 S2). Next we studied the expression pattern of *GA3ox1*, which catalyses the last step in
298 the biosynthesis of bioactive GA₁ and GA₄ (Talon et al., 1990). Expression was
299 significantly increased in developing ovules of the *ats-1* mutant (Fig. 5B). The
300 increased *GA3ox1* expression in *ats-1* likely led to increase bioactive GAs, which
301 finally might promote the alteration in ovule morphology. To analyze whether the
302 increased GA content affected DELLA protein stability in ovules, we tested the RGA
303 levels using the *pRGA:RGA-GFP* reporter construct (Silverstone et al., 2001). While
304 RGA was located in the chalaza and integuments of developing ovules, levels were
305 decreased in the *ats-1* mutant (Fig. 5C). Furthermore, RGA-GFP levels were also
306 decreased in both secondary roots, where ATS is also expressed (Hawker et al., 2004),
307 and the primary root (Supplemental Figure S3). In conclusion, our data indicated a role
308 of ATS in repressing GA synthesis; low GA levels would stabilize DELLAs to properly
309 coordinate growth and development. The increased GA biosynthesis in *ats-1* would
310 result in DELLA degradation and the deregulation of GA-controlled processes,
311 including germination, flowering time, or ovule development.

312

313

314 **DELLAs interact with ATS**

315 DELLAs function as transcriptional regulators, but do not encode any known
316 DNA-binding domain. This role is exerted through their interaction with TFs. KAN1, a
317 related KANADI gene family member, has been recently described as a putative
318 DELLA interacting protein (Marin-de la Rosa et al., 2015). Therefore, a plausible

Figure 5. Gomez et al.

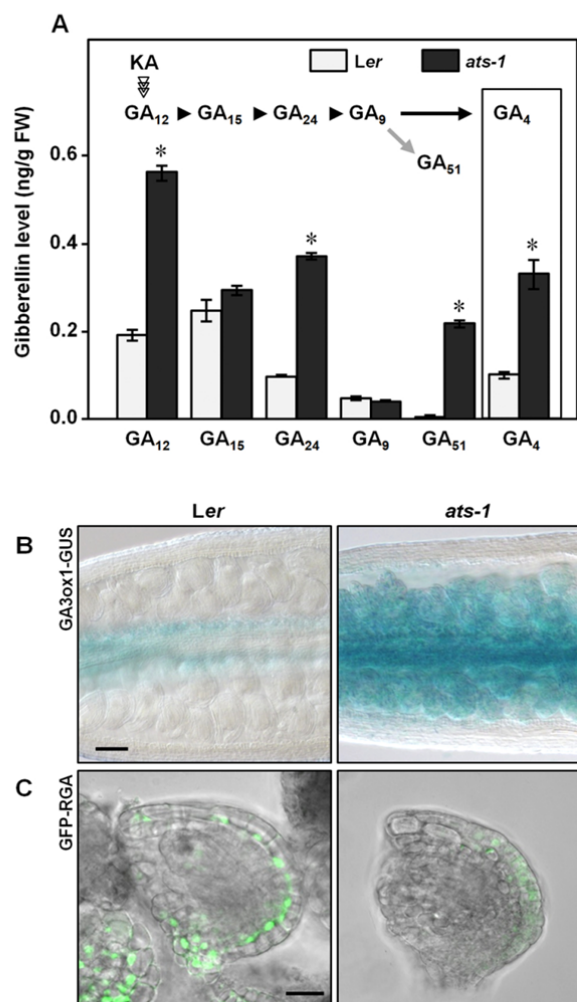


Figure 5. GA levels increased in *ats-1*.

A, The levels of GAs in the GA₄ pathway in *Ler* (gray) and *ats-1* (black). The GA₄ synthesis pathway is indicated: KA, ent-kaurenoic acid; black arrow head, GA₂₀oxidase; black arrow, GA₃oxidase; gray arrow, GA₂oxidase. Significant differences (Student's t-test analysis) between *Ler* and *ats-1* are indicated by an asterisk (*, p-value < 0.001). Data are the mean±SE of three independent samples, expressed as ng of GA per g of FW. **B**, Expression of GA biosynthesis gene *GA3ox1* by reporter pGA_{3ox1}:GA_{3ox1}-GUS in ovule primordia at stage 3-I of *Ler* and *ats-1*. **C**, GFP-RGA protein stability in ovule primordia of *Ler* and *ats-1* at stage 3-III. Scale bars represent 100 μm in B, and 20 μm in C and D.

319 hypothesis would be that ATS/KAN4 could also interact with the DELLA proteins. To
 320 address this hypothesis, we performed a yeast two-hybrid assay using truncated versions
 321 of GAI and RGA, which prevent the auto-activation of reporter genes (de Lucas et al.,
 322 2008) and ATS. The *ATS* locus encodes at least two splice variants: ATS.1, the longest

Figure 6. Gomez et al.

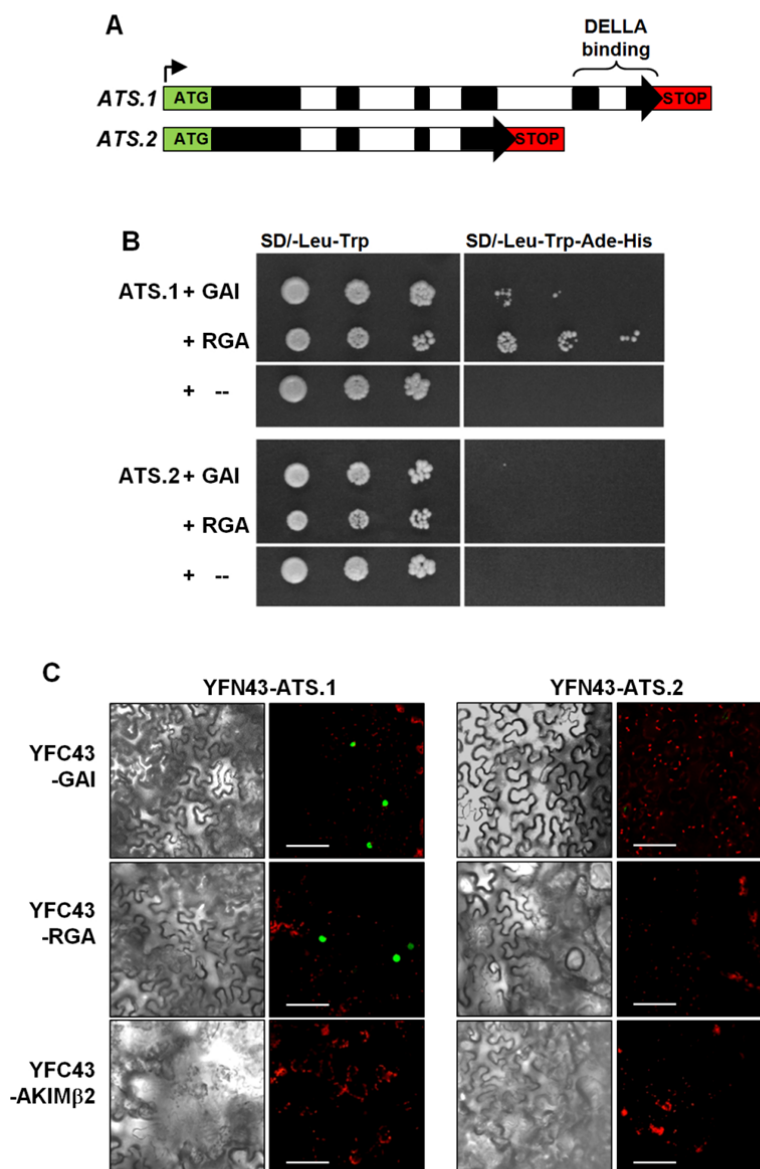


Figure 6. ATS directly binds to DELLAs.

A, Gene structure of the *ATS.1* and *ATS.2* splicing variants. The putative domain required for binding is localized in the 5 and 6 exons of *ATS.1*. **B**, Yeast two hybrid assay. DELLAs GAI and RGA fused to Gal4 DNA-BD were tested with *ATS.1* and *ATS.2* full-length ORFs fused to Gal4 DNA-AD. Diploids were grown in the SD/-Leu-Trp and SD/-Leu-Trp-His-Ade medium. **C**, BiFC assay. Full length GAI and RGA in pYFC43 were assayed with *ATS.1* and *ATS.2* in pYFN43. AKIMβ2 in pYFC43 was used as a negative control (Belda-Palazon et al., 2012). Left panels are the bright field image and right panels are the merged image of chlorophyll and YFP. Scale bar represent 100 μm.

323 with 6 exons, and *ATS.2*, which lacks the last two exons (Fig. 6A) (Gao et al., 2010).
 324 Interaction assays demonstrated that only *ATS.1* was able to interact with GAI and
 325 RGA (Fig. 6B). No interaction was observed for truncated version *ATS.2*, which
 326 indicated that the last 67 amino acids at the carboxyl end of *ATS.1* are an absolute

327 requirement for DELLA-ATS binding, and either act as the binding domain or stabilize
328 the DELLA-ATS interaction. This domain does not encode for any known canonical
329 protein motif. On the other hand, we also confirmed that GAI and RGA could also bind
330 to KAN1 (Supplemental Fig. S4). We examined the subcellular localization of the GAI-
331 ATS and RGA-ATS interactions by Bimolecular Fluorescence Complementation
332 (BiFC) and found that the reconstructed YFP protein was observed only in the nuclei of
333 epidermal cells that co-expressed YFP-ATS.1 and YFP-GAI or YFP-RGA (Fig. 6C and
334 Supplemental Fig. S5). As in the yeast assay, ATS.2 did not bind to GAI or RGA in
335 plants. This further confirmed the DELLA-ATS interaction *in vivo*.

336 If DELLA proteins regulate integument development it is necessary that they are
337 expressed in these tissues, along with ATS. All four DELLAs *GAI*, *RGA*, *RGL1* and
338 *RGL2* were expressed in developing ovules (Fig. 7B), but with gene-specific patterns:
339 *GAI* expression was located mainly in the funiculus, but also in integument primordia
340 and in the center of the nucellus; *RGA* and *RGL1* were expressed in the funiculus and
341 integument primordia; and *RGL2* was expressed preferentially in the nucellus but also
342 in the integument and funiculus. Therefore, the four DELLAs that were genetically
343 involved in ovule development seemed expressed in the integuments during
344 development, in the same tissues where *ATS* is expressed (Supplemental Fig. S6A)
345 (McAbee et al., 2006), as well as in other tissues within the ovule.

346

347

348 **ATS expression in integuments during ovule development is not regulated by GAs.**

349 We also interrogated whether *ATS* and *DELLAs* regulate each other at the
350 transcriptional level. First, we tested that there were no differences in the expression of
351 *ATS* in the WT and *global* ovules (Supplementary Fig. S6A). In both cases, *ATS*
352 expression was observed in the abaxial cells of the inner integument and in the adaxial
353 cells of the outer integument in developing ovules, as it was previously reported
354 (McAbee et al., 2006). The qPCR analysis revealed that *ATS* was expressed at similar
355 levels in both inflorescences and seedlings of the *global* mutant and WT (Supplemental
356 Fig. S6B), which confirmed *in situ* hybridization data. On the other hand, the expression

Figure 7. Gomez et al.

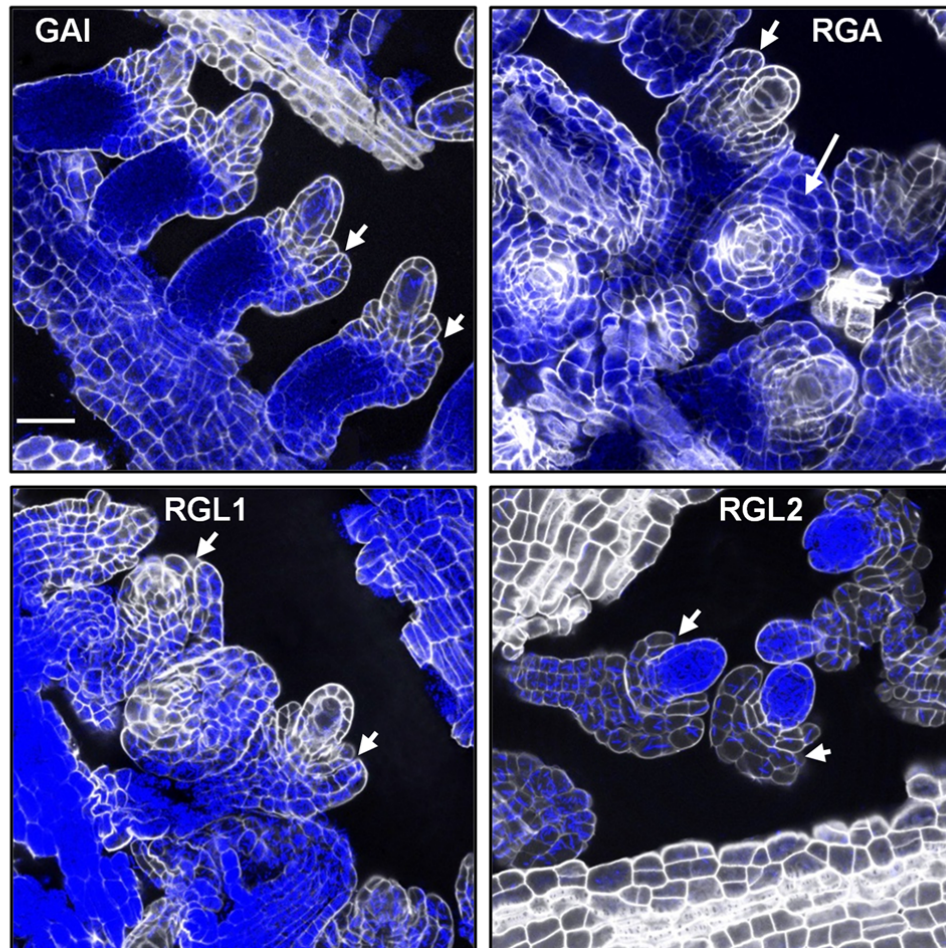


Figure 7. DELLAs are expressed in ovule integuments. Expression of DELLAs by GUS assay coupled with mPS-PI staining. *GAI*, *RGA* and *RGL1* were detected with transcription lines p*GAI*:GUS, p*RGA*:GUS, and p*RGL1*:GUS (Gallego-Giraldo et al., 2014). Expression of *RGL2* was monitored using the *rgl2-5* allele (Lee et al., 2002). Scale bar represents 20 μ m.

357 of DELLA genes *GAI* and *RGA* was not significantly affected in either the seedlings or
358 inflorescences of *ats-1* (Supplemental Fig. S6C). We conclude from these results that
359 DELLA proteins would not be involved in the regulation of *ATS* expression and that
360 *ATS* would not regulate DELLA gene expression. Therefore, it seems that no reciprocal
361 transcriptional regulation exists between *ATS* and DELLAs.

362

363

364 **Both *ATS* and DELLA functions are required for correct ovule development**

365 The similar phenotypes of the loss-of-function of ATS and DELLA and the
366 physical interaction showed herein suggested that presence of a protein complex
367 participated by both proteins could be a strict requirement for correct ovule
368 development. Regardless of the interaction capacity of ATS to DELLA, elevated GA
369 levels in *ats-1* could be the cause of the described ovule defects; increased GA levels
370 would result in the destabilization of DELLAs and would, hence, promote similar ovule
371 defects to those in the *global* mutant. In this scenario, a dominant DELLA in an *ats-1*
372 background would overcome ovule defects by reestablishing the proper DELLA
373 function. As observed in Figure 8, the gain-of-function of DELLA in the *gai-1* mutant
374 did not rescue the ovule and seed phenotypes of *ats-1*, which supports the notion that
375 both ATS and DELLAs have to be present to promote integument differentiation. While
376 *gai-1* showed elongated seeds, the double *gai-1 ats-1* had round seeds that were similar
377 in shape and length/width ratio to those from *ats-1* (Fig. 8). In addition, the seeds of the
378 double *ats-1 gai-1* showed viviparism, as in the single *ats-1* and the *global* mutant (Fig.
379 8A, inset). In contrast, the overall seed size of *gai-1 ats-1* was somewhat larger than
380 those from the single *ats-1* (Fig. 8, B and C), which indicated that the gain-of-function
381 of GAI may promote cell elongation in both the major and minor axes of seeds (Vivian-
382 Smith and Koltunow, 1999). The fact that the dominant *gai-1* was unable to overcome
383 ovule defects in *ats-1* implies that the ATS-DELLA physical protein interaction may be
384 the molecular mechanism by which GAs play a role in integument development.

385

386

387

Figure 8. Gomez et al.

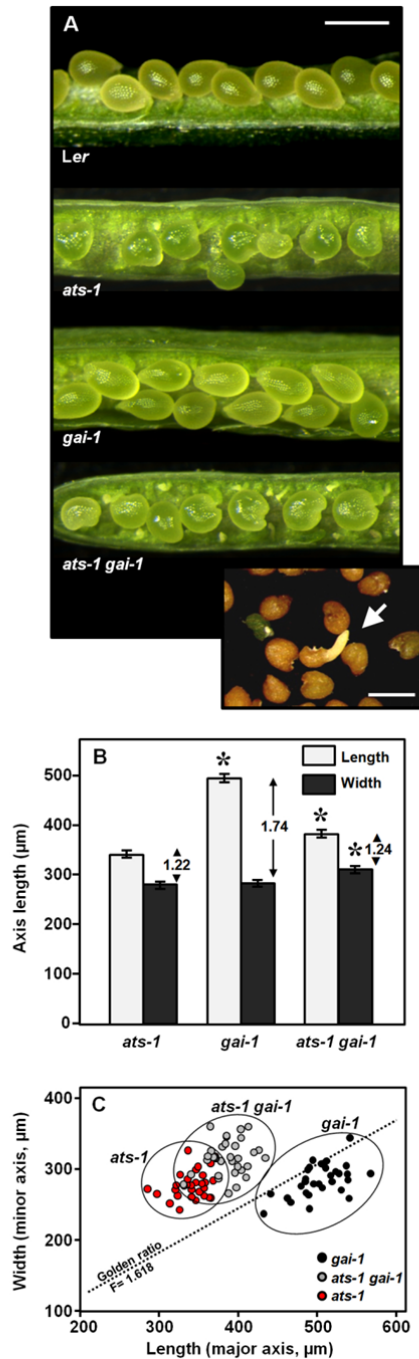


Figure 8. Gain-of-function of DELLA activity does not rescue the *ats-1* mutant defects in seed development.

A, Images of 8-dpa fruits from *Ler* and the *ats-1*, *gai-1*, and double *ats-1 gai-1* mutants. The white arrow marks a viviparous *ats-1 gai-1* seed. Scale bars represent 500 μm. **B**, Seed length and width of *gai-1*, *ats-1*, and double *ats-1 gai-1*. Data are the mean±SE of three biological replicas, each one from 25-30 seeds. Significant differences (Student's *t*-test analysis) are marked with asterisks, and *ats-1* is taken as a reference (* *p*-value < 0.01). The seed length and width ratio is indicated. **C**, Size distribution of the mature seeds of the *ats-1*, *gai-1* and double *ats-1 gai-1*, represented as length (major axis) and width (minor axis). Golden ratio is represented by a line at the 1.618 ratio.

388 DISCUSSION

389 In this study we report the role of GAs in the control of integument development
 390 during ovule ontogenesis. Our data indicate that DELLA proteins play an essential role

Figure 9. Gomez et al.

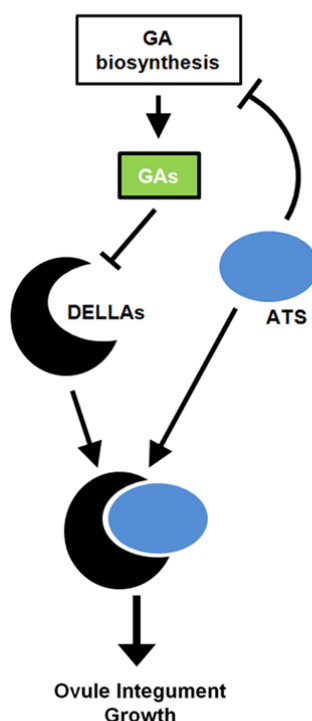


Figure 9. Model for the ATS and DELLA interaction in the control of ovule development. ATS and DELLA directly bind in ovule primordia to mediate proper ovule development, probably by regulating the expression of the genes required for ovule development. In addition, ATS inhibits GA biosynthesis, which promotes low GA levels and the stabilization of DELLAs to facilitate the formation of the protein complex.

391 in the correct formation of ovule integument, while constitutive GA signaling has
392 detrimental effects. The similarity of the *global* and *ats-1* mutant phenotypes strongly
393 suggests that both DELLAs and ATS participate in integument growth during late
394 stages of ovule ontogeny via a common molecular mechanism (Fig. 9). ATS and
395 DELLAs interact to coordinate proper ovule growth. This function would require the
396 presence of both proteins in a complex, and would explain why the absence of either of
397 them in the *global* or *ats-1* mutants results in similar ovule and seed phenotypes. In line
398 with this, GA biosynthesis repression by ATS may promote the stabilization of
399 DELLAs, which would strengthen the protein complex (Fig. 9). The fact that *ats-1* but
400 not *global* shows fused integuments from early stages, would indicate that the role of
401 ATS in this phase of development would not require the activity of DELLAs. Likewise,
402 DELLAs would also have roles in ovule and seed development in other tissues where
403 ATS is not active.

404 DELLAs can modulate transcription by binding to TFs in the promoter of target
405 genes (Marin-de la Rosa et al., 2015; Daviere and Achard, 2016). It has recently

406 reported that RGA was localized at *cis* elements that are potential binding motifs of the
407 GARP-G2 TFs, that include ATS/KAN4 and KAN1 (Franco-Zorrilla et al., 2014;
408 Marin-de la Rosa et al., 2015). These data strongly suggest that ATS could recruit
409 DELLAs to the promoters of the ATS target genes involved in integument growth
410 through direct protein-protein interaction. In addition, the binding ATS and DELLA in
411 ovule development resembles that of DELLAs and other GARP genes, the type-B
412 ARABIDOPSIS RESPONSE REGULATORS (ARRs) in root growth. In this case RGA
413 binds to ARR1 in the promoters of cytokinin-regulated genes, acting as transcriptional
414 co-activators (Marin-de la Rosa et al., 2015). This molecular mechanism depends on the
415 necessity of the simultaneous presence of DELLAs and ARR1 to restrict root meristem
416 growth and to promote photomorphogenesis, similarly to the DELLA-ATS function in
417 ovule integument. RGA selectively induces the expression of ARR1 in the meristem
418 (Moubayidin et al., 2010), which may contribute to facilitate ARR1-DELLA complex
419 formation to arrest meristem growth. In contrast, the expression of DELLAs is not
420 regulated by ATS, or vice versa. In the case of the integument, repression of GA
421 biosynthesis by ATS would stabilize DELLA proteins and favors the ATS-DELLA
422 complex formation.

423 ATS also interacts with ETT/ARF3 to define the boundary between the
424 integument primordia in the ovule (Kelley et al., 2012). The loss-of-function ATS or
425 ETT resulted in common defects in ovule integument development and seed shape,
426 probably by altering auxin distribution in ovule primordia. Interestingly, DELLAs can
427 also bind to ETT (M. Blazquez and D. Alabadi, unpublished), which points out to a
428 multicomplex protein DELLA-ATS-ETT that could coordinate ovule growth and
429 development.

430 Early seed germination within siliques was observed in the *global* and *ats-1*
431 mutants. It is well known that GAs and ABA play antagonistic roles in seed
432 dormancy/germination by means of a dynamic balance between the synthesis and
433 catabolism of these two hormones (Gutierrez et al., 2007; Holdsworth et al., 2008;
434 Weitbrecht et al. 2011). On the other hand, reduced dormancy could be a direct
435 consequence of the diminished mechanical resistance in the testa caused for the loss-of
436 function of the DELLA-ATS complex. It is difficult to discriminate whether viviparism
437 is merely the consequence of testa defects or the result of the constitutive GA signaling
438 (*global*) or elevated GA levels (*ats-1*). However, viviparism was still observed in the
439 double *ats-1 gai-1*, which has blocked the GAI-dependent GA signaling, suggesting that

440 defects in the testa of *ats-1* are potentially responsible for the reduced dormancy. *ats-1*
441 also showed early germination and advance flowering, similarly to the *global* mutant.
442 Whether these phenotypes are the effect of the elevated GA levels or due to a specific
443 role of ATS-DELLA, as it was observed in ovule development, needs further study.

444 In conclusion, we have shown that the correct control of GA/DELLA levels is
445 necessary to achieve proper integument development and to generate a normal testa in
446 mature seeds. Constitutive GA signaling by diminished DELLA function results in
447 changes in the ovule/seed shape due to alterations in integuments/testa, which have
448 consequences in both fertility and seed dormancy.

449 MATERIALS AND METHODS

450

451 Plant material assays for fruit-set, parthenocarpy, germination and flowering.

452 Seeds were surface-sterilized in EtOH, plated onto MS media (Murashige and
453 Skoog, 1962), incubated at 4°C for 4 days in complete darkness, and transferred to a
454 growth chamber at 22°C in long day photoperiod (16/8h) for 10 days. Seedlings were
455 transferred to soil (a mix of peat moss, vermiculite and perlite, 2:1:1) and grown in a
456 growth chamber at 22°C in long day photoperiod.

457 *ats-1* was obtained from the NASC. The *della global* mutant (*quintuple gai-t6*
458 *rga-t2 rgl1-1 rgl2-1 rgl3-1*) (Feng et al., 2008) was obtained from SW Deng (Yale
459 University, US). Triple DELLA mutants *gai-t6 rga-24 rgl1-1*, *gai-t6 rga-24 rgl2-1*, *gai-*
460 *t6 rgl1-1 rgl2-1*, and *rga-24 rgl1-1 rgl2-1* were obtained by genetic cross from single
461 mutants. The pDELLA:GUS lines have been previously reported (Gallego-Giraldo et
462 al., 2014). The pRGA:GFP-RGA (Silverstone et al., 2001) and pGA3ox1:GA3ox1-GUS
463 lines (Mitchum et al., 2006) were obtained from T-p. Sun (Duke University, USA).

464 Fertility was assayed in hand-emasculated flowers 1 day before anthesis and
465 hand pollinated with WT pollen at anthesis. Fruits were collected at maturity (14 days
466 post-anthesis, dpa), seed number was counted and silique length was measured with a
467 digital caliper. The ratio (seed number vs. silique length) was determined.
468 Parthenocarpy was assayed in hand-emasculated flowers, which were not pollinated.

469 Germination was assayed in 2-3-week old seeds, plated in MS, stratified for 3
470 days at 4°C in the darkness. Germination was scored 3 days after incubation at 22°C as
471 radicle emergence through the testa. Flowering was assayed under long-day (LD, 16/8h)
472 and short-day (SD, 8/16h) conditions. After stratifying for 3 days at 4°C in the darkness,

473 seeds were germinated directly in soil and grown at 22°C. The total number of leaves
474 before flowering was scored.

475

476 **Gene expression analysis by qPCR**

477 Three-day old seedlings and inflorescences were used. Total RNA was
478 extracted with the RNeasy Plant Mini Kit (Qiagen) and genomic DNA was eliminated
479 with DNase I (Qiagen). cDNA was synthesized using the SuperScript First-Strand
480 Synthesis System for RT-PCR (Invitrogen) and qPCR was carried out with the SYBR[®]
481 GREEN PCR Master Mix (Applied Biosystems) with an ABI PRISM 7000 Sequence
482 Detection System (Applied Biosystems), as previously described (Dorcey et al., 2009).
483 Expression levels were calculated according to the expression of the constitutive
484 *EIF4A1* (*At3g13929*) and data were normalized by the $\Delta\Delta C_t$ method. The primers for
485 the splicing version ATS.1 (Forward 5'-CAACTCATCACACTAAGGACAATGAAG-
486 3', which spanned the intron between exon 5 and 6, and Reverse oligo 5'-
487 CCAAATTGAGATGAATGTTGGTATCC-3') were tested for efficiency. The primers
488 for GAI, RGA, and GA biosynthesis genes were previously described (Dorcey et al.,
489 2009; Gallego-Giraldo et al., 2014).

490

491 **Scanning Electron Microscopy (SEM)**

492 Seeds were mounted on SEM stubs attached to the specimen holder of a CT-
493 1000C cryo-transfer system (Oxford Instruments), and frozen in liquid N₂. The frozen
494 samples were transferred to the cryo-stage of a JEOL JSM-5410 scanning electron
495 microscope, sublimated at -85°C, and sputter coated with a film of gold. Finally,
496 samples were observed at incident electron energy of 10 kV.

497

498 **Histological procedures**

499 The pGA3ox1:GA3ox1-GUS (Mitchum et al., 2006) and pDELLA:GUS lines
500 (Gallego-Giraldo et al., 2014) were used for the GUS assay and the histological
501 procedures basically as previously described (Carbonell-Bejerano et al., 2010). The
502 K₃Fe(CN)₆ and K₄Fe(CN)₆ concentrations were adjusted for each line to obtain optimal
503 signals (5 mM for pGAI:GUS and pRGA:GUS; 2 mM for pRGL1:GUS, and 4 mM for
504 *rgl2-5*, and 50 μ M for pGA3ox1:GA3ox1-GUS). After GUS staining, samples were
505 either cleared with chloral hydrate or stained following a modified pseudo-Schiff
506 propidium iodide (mPS-PI) technique (Truernit et al., 2008). Images were captured with

507 a microscope Eclipse E600 (Nikon) equipped with Nomarski interference optics or with
508 a ZEISS LSM 780 confocal microscope. GUS staining was visualized in the confocal
509 with a MBS T80/R20 dichroic (561 nm and 545-570 nm excitation and reflexion,
510 respectively). PI staining was excited at 561 nm and detected at 580-660 nm.

511 For thin sectioning in Figure 3D and E, fruits were fixed overnight in 4% (w/v)
512 p-formaldehyde in 0.1 M sodium phosphate, pH 7.2, with 0.05% (v/v) of Tween 20 at
513 4°C and dehydrated in ethanol. Samples were then infiltrated in Technovit 7100 resin,
514 sectioned in a Reichert Jung Ultracut E microtome at 3 µm, and stained in 0.02%
515 Toluidine blue as described in Gomez et al. (2004).

516

517 **Quantification of GAs**

518 GAs were quantified basically as described by Seo et al. (2011). Three-day-old
519 seedlings were extracted with 80% methanol-1% acetic acid, and extracts were passed
520 consecutively through HLB (reverse phase), MCX (cationic exchange) and WAX (ionic
521 exchange) columns (Oasis 30 mg, Waters). GAs were separated using reverse phase
522 UPHL chromatography (2.6 µm Accucore RP-MS column; ThermoFisher Scientific)
523 with a 5-50% acetonitrile gradient with 0.05% acetic acid at 400 µL/min. GAs were
524 analyzed by electrospray ionization and targeted-SIM in a Q-Exactive spectrometer
525 (Orbitrap detector; ThermoFisher Scientific). [17,17-²H] GA₄, GA₉, GA₁₂, GA₁₅, GA₂₄,
526 GA₃₄ and GA₅₁ were used as internal standards for quantification.

527

528 ***In situ* RNA hybridization**

529 Inflorescences were embedded, sectioned and hybridized as described
530 elsewhere (Weigel and Glazebrook, 2002; Gomez et al., 2011). The partial clone for
531 ATS.1, corresponding to the complete codifying sequence, was cloned in the pGEM-T
532 easy vector (Promega). Sense and antisense probes were synthesized using the SP6 and
533 T7 RNA polymerases, respectively.

534

535 **Yeast two hybrid.**

536 Full-length ORFs were first cloned in pGEM-T (ATS.1 and ATS.2) or pBSK
537 (KAN1), and transferred into pGADT7 (Clontech) by EcoRI-ClaI digestion-ligation.
538 The M5-truncated versions of cDNA for GAI and RGA (de Lucas et al., 2008) in
539 pGBKT7 (Clontech) were obtained from S. Prat (CNB, Spain). Plasmids pGADT7 and
540 pGBKT7 were introduced into the Y187 and the Y2HGold yeast strain, respectively.

541 Both strains containing the corresponding plasmids were mated o/n at 28°C and diploids
542 were selected in the SD media supplemented with His and Ade. The interaction was
543 assayed on minimal media plates without either Leu/Trp or Leu/Trp/Ade/His in 10-fold
544 serial dilutions for 5 days at 28°C. Empty vectors were used as negative controls.

545

546 **BiFC assay.**

547 The BiFC assay was carried out basically as described in Belda-Palazon et al.
548 (2012). The full-length ORFs of ATS.1/ATS.2 and GAI/RGA were cloned in pCR8 and
549 transferred by GATEWAY into the YFN43 and the YFC43 plasmid, respectively. As a
550 nonspecific control, cDNAs for AKIN β 2 in pYFC43 and AKIN10 in pYFN43 were
551 used (Ferrando et al., 2001). Fluorescence was observed 2-3 days after infiltration at
552 488 nm under a ZEISS LSM 780 confocal microscope.

553

554

555 **ACKNOWLEDGMENTS**

556 We wish to thank Dr. T-p. Sun (Duke University) for the pGA3ox1:GA3ox1-
557 GUS and pRGA:GFP-RGA lines, Dr. S.W. Deng (Yale University) for the *global*
558 mutant, Dr. S. Prat (CNB, Spain) for the M5-truncated versions of GAI and RGA in
559 pGBKT7, and Dr. A. Ferrando (IBMCP, Spain) for the BiFC plasmids. We also thank
560 Dr. I. Lopez-Diaz and E. Carrera (hormone quantification facility, IBMCP, Spain) for
561 the quantification of GAs, and Ms. M. Gascon, C. Fuster and M.A. Argomániz for
562 technical assistance.

563

564

565 **FIGURE LEGENDS**

566

567 **Figure 1. Constitutive GA signaling in the *della global* mutant causes seed defects**
568 **and reduced fertility, similarly to *ats-1*.**

569 **A**, Silique length, seed number, and length/width ratio in fruits of *Ler* and the *global*
570 and *ats-1* mutants at 12 days-post-anthesis (dpa). Data are the mean and standard error
571 (SE) of three independent experiments, each one from at least 50 fruits. The significant
572 differences (Student's *t*-test analysis) between *Ler* and mutants are marked with
573 asterisks (* *p*-value < 0.01). **B-C**, Images of whole (**B**) and open (**C**) 8-dpa fruits of *Ler*,
574 and the *global* and *ats-1* mutants. **D-E**, Images of mature seeds of *Ler*, and the *global*
575 and *ats-1* mutants, taken by SEM (**D**) or stereomicroscope (**E**). The white arrow marks
576 the viviparous seeds of the *ats-1* and *global* mutants. All the images in each category
577 have the same magnification. Scale bars represent 2 mm in B, 500 μ m in C and E, and
578 100 μ m in D.

579

580 **Figure 2. DELLAs and ATS regulate seed size and shape.**

581 **A**, SEM images of mature seeds of *Ler* and the *gai-1* mutant. Length and width (major
582 and minor axis, respectively) are marked with white arrows in *Ler* seed. **B**, Size
583 distribution of mature seeds of *Ler* and the *gai-1*, *global* and *ats-1* mutants, represented
584 as length (major axis) and width (minor axis). Golden ratio is represented by a line at
585 the 1,618 ratio. **C**, Seed length and width of *Ler* and the *gai-1*, *global*, and *ats-1*
586 mutants. Data are the mean \pm SE of three biological replicas, each one from 25-30 seeds.
587 Significant differences (Student's *t*-test analysis) between *Ler* and mutants are marked
588 with asterisks (* *p*-value < 0.01). The ratio between seed length and width is indicated.

589

590 **Figure 3. DELLAs and ATS regulate ovule integument development.**

591 **A-B**, Images of *Ler*, *global* and *ats-1* ovules at stage 2-III (**A**) and 3-II (**B**) (Schneitz et
592 al., 1995). **C**, Images of ovules at anthesis. The shape of the embryo sac (es) is marked
593 by blue lines. **D-E**, Transversal section of the fertilized ovules at 3 dpa (**D**) or 7 dpa (**E**).
594 The outer and inner integument layers of WT in A and D are indicated with asterisks
595 and dots, respectively. Scale bars represent 50 μ m in A, B and C and 100 μ m in D and
596 E.

597

598 **Figure 4. *ats-1* shows higher seed germination and early flowering.**

599 **A**, Germination rate of *Ler* and the *ats-1*, *global*, and *rgl2-1* mutants. Germination was
600 scored at 3 days in the absence (-PCB) or presence of 1 μ M of PCB (+PCB). **B**,
601 Flowering time of *Ler* and the *ats-1* and *global* mutants. Flowering was scored as the
602 number of leaves in plants grown in long (LD) and short (SD) days. Significant
603 differences (Student's *t*-test analysis) between *Ler* and mutants are indicated by an
604 asterisk (*, *p*-value < 0.01). Data are the mean \pm SE of three biological replicas, each one
605 from 80-100 seeds in A and 30-40 plants in B.

606

607 **Figure 5. GA levels increased in *ats-1*.**

608 **A**, Levels of GAs in the GA₄ pathway in *Ler* (gray) and *ats-1* (black). The GA₄
609 synthesis pathway is indicated: KA, ent-kaurenoic acid; black arrow head,
610 GA20oxidase; black arrow, GA3oxidase; gray arrow, GA2oxidase. Significant
611 differences (Student's *t*-test analysis) between *Ler* and *ats-1* are indicated by an asterisk
612 (*, *p*-value < 0.001). Data are the mean \pm SE of three independent samples, expressed as
613 ng of GA per g of FW. **B**, Expression of GA biosynthesis gene *GA3ox1* by reporter
614 pGA3ox1:GA3ox1-GUS in developing ovules at stage 3-I of *Ler* and *ats-1*. **C**, GFP-
615 RGA protein stability in integuments of *Ler* and *ats-1* at stage 3-III. Scale bars represent
616 100 μ m in B, and 20 μ m in C and D.

617

618 **Figure 6. ATS directly binds to DELLAs.**

619 **A**, Gene structure of the ATS.1 and ATS.2 splicing variants. The putative domain
620 required for binding is localized in the 5 and 6 exons of ATS.1. **B**, Yeast two hybrid
621 assay. DELLAs GAI and RGA fused to Gal4 DNA-BD were tested with ATS.1 and
622 ATS.2 full-length ORFs fused to Gal4 DNA-AD. Diploids were grown in the SD/-Leu-
623 Trp and SD/-Leu-Trp-His-Ade medium. **C**, BiFC assay. Full length GAI and RGA in
624 pYFC43 were assayed with ATS.1 and ATS.2 in pYFN43. AKIM β 2 in pYFC43 was
625 used as a negative control (Belda-Palazon et al., 2012). Left panels are the bright field
626 image and right panels are the merged image of chlorophyll and YFP. Scale bar
627 represent 100 μ m.

628

629

630

631 **Figure 7. DELLAs are expressed in ovule integuments.**

632 Expression of DELLAs by GUS assay coupled with mPS-PI staining. *GAI*, *RGA*, and
633 *RGL1* were detected with transcription lines pGAI:GUS, pRGA:GUS, and pRGL1:GUS
634 (Gallego-Giraldo et al., 2014). Expression of *RGL2* was monitored using the *rgl2-5*
635 allele (Lee et al., 2002). Scale bar represents 20 μ m.

636

637 **Figure 8. Gain-of-function of DELLA activity does not rescue the *ats-1* mutant**
638 **defects in seed development.**

639 **A**, Images of 8-dpa fruits from *Ler* and the *ats-1*, *gai-1*, and double *ats-1 gai-1* mutants.
640 The white arrow marks a viviparous *ats-1 gai-1* seed. Scale bars represent 500 μ m. **B**,
641 Seed length and width of *gai-1*, *ats-1* and double *ats-1 gai-1*. Data are the mean \pm SE of
642 three biological replicas, each one from 25-30 seeds. Significant differences (Student's
643 *t*-test analysis) are marked with asterisks, and *ats-1* is taken as a reference (* p-value <
644 0.01). The seed length and width ratio is indicated. **C**, Size distribution of the mature
645 seeds of the *ats-1*, *gai-1*, and double *ats-1 gai-1* mutants, represented as length (major
646 axis) and width (minor axis). Golden ratio is represented by a line at the 1,618 ratio.

647

648 **Figure 9. Model for the ATS and DELLA interaction in the control of ovule**
649 **development.**

650 ATS and DELLA directly bind to mediate proper ovule development, probably by
651 regulating the expression of the genes required for ovule development. In addition, ATS
652 inhibits GA biosynthesis, which promotes low GA levels and the stabilization of
653 DELLAs to facilitate the formation of the protein complex.

654

655 **Supplemental Data**

656 **Supplemental Figure S1. Parthenocarpy and seed defects are characteristic of the**
657 ***global* and *quadruple*, but not of any of the triple *della* null mutants.**

658 **Supplemental Figure S2. Expression analysis of GA biosynthesis genes.**

659 **Supplementary Figure S3. Increased GA level in *ats-1* promotes RGA degradation**
660 **in roots.**

661 **Supplemental Figure S4. Binding of GAI and RGA to KAN1 in yeast two hybrid**
662 **assay.**

663 **Supplemental Figure S5. Controls of the BiFC assay between DELLAs with ATS.**

664 **Supplemental Figure S6. ATS and DELLAs do not regulate each other at the**
665 **transcriptional level.**

666

667

668

669 **Supplemental Figure S1. Parthenocarpy and seed defects are characteristic of the**
670 ***global* and *quadruple*, but not of any of the triple *della* null mutants.** **A,** Fruit/pistil
671 length of WT, *global* and the triple mutant combinations of *GAI*, *RGA*, *RGL1* and
672 *RGL2*. Flowers were hand-emasculated and fruit or pistil length was scored at 12 dpa.
673 Data are the mean±SE of three independent experiments, each one from 40-50 flowers.
674 Significant differences (Student's *t*-test analysis) between *Ler* and mutants are marked
675 with asterisks (* *p*-value < 0.01). **B,** Images of 8-dpa fruits of *Ler* and the *global*,
676 *quadruple*, and triple DELLA mutants. **C,** Genotype of the *della* mutants used in this
677 assay. Triple 1 (t1) is *gaiT6 rga24 rgl1-1* with native RGL2; triple 2 (t2) is *gaiT6 rga24*
678 *rgl2-1* with native RGL1; triple 3 (t3) is *gaiT6 rgl1-1 rgl2-1* with native RGA; triple 4
679 (t4) is *rga24 rgl1-1 rgl2-1* with native GAI. Scale bar represents 500 µm.

680

681 **Supplemental Figure S2. Expression analysis of GA biosynthesis genes.**

682 qPCR expression analysis of *GA20ox1*, *GA20ox2*, *GA3ox1* and *GA3ox2* in 3-day-old
683 seedling of *Ler* (light gray) and the *ats-1* (dark gray). Expression was normalized to that
684 of *EIF4A1* (*At3g13929*) in *Ler*. Data are the mean±SE of three biological replicas.

685

686 **Supplementary Figure S3. Increased GA level in *ats-1* promotes RGA degradation**
687 **in roots.**

688 GFP-RGA protein stability in secondary (A) and primary (B) roots of *Ler* and *ats-1* of
689 3-day old seedlings. Scale bar represents 30 µm.

690

691 **Supplemental Figure S4. Binding of GAI and RGA to KAN1 in yeast two hybrid**
692 **assay.**

693 **A-B,** Yeast two hybrid assay of the M5-truncated version of GAI, RGA, and the
694 pGBKT7 empty vector (BD, --) against KAN1 (A) or the pGADT7 empty vector (AD, -
695 -) (B).

696

697 **Supplemental Figure S5. Controls of the BiFC assay between DELLAs with ATS.**

698 Upper panel, nonspecific protein AKIN10 in pYFN43 was assayed with RGA in
699 pYFC43. Medium panel, the empty pYFN43 vector was assayed with GAI and RGA in

700 pYFC43. Lower panel, BiFC assay using empty pYFN43 and pYFC43 vectors. No
701 signal was observed in any plasmid combination. BF, bright field; merge, merged
702 images of chlorophyll and YFP. Scale bar represents 100 μm .

703

704 **Supplemental Figure S6. *ATS* and *DELLAs* do not regulate each other at the**
705 **transcriptional level.**

706 **A**, *In situ* mRNA hybridization of *ATS* in the ovules of *Ler* and the *global* mutant at
707 stage 2-III. Outer and inner integument cell layers are indicated with black and blue
708 asterisks, respectively. **B**, Expression of *ATS* in 3-day old seedlings and inflorescences
709 of *Ler* (light gray) and the *global* mutant (dark gray). **C**, Expression of *GAI* and *RGA* in
710 3-day-old seedling of *Ler* (light gray) and *ats-1* (dark gray). The expression of *ATS* and
711 *DELLAs* in B and C was normalized to that of *EIF4A1* (*At3g13929*) in *Ler*. Data are the
712 mean \pm SE of three biological replicas.

713

714

715

716

717

Parsed Citations

Abramoff MD, Magelhaes PJ, Ram SJ (2004) Image Processing with ImageJ. Biophot Int 11: 36-42

Pubmed: [Author and Title](#)

CrossRef: [Author and Title](#)

Google Scholar: [Author Only](#) [Title Only](#) [Author and Title](#)

Arnaud N, Girin T, Sorefan K, Fuentes S, Wood TA, Lawrenson T, Sablowski R, Ostergaard L (2010) Gibberellins control fruit patterning in Arabidopsis thaliana. Genes Develop 24: 2127-2132

Pubmed: [Author and Title](#)

CrossRef: [Author and Title](#)

Google Scholar: [Author Only](#) [Title Only](#) [Author and Title](#)

Asano K, Hirano K, Ueguchi-Tanaka M, Angeles-Shim RB, Komura T, Satoh H, Kitano H, Matsuoka M, Ashikari M (2009) Isolation and characterization of dominant dwarf mutants, Slr1-d, in rice. Mol Genet Genomics 281: 223-231

Pubmed: [Author and Title](#)

CrossRef: [Author and Title](#)

Google Scholar: [Author Only](#) [Title Only](#) [Author and Title](#)

Bassel GW, Mullen RT, Bewley JD (2008) Procera is a putative DELLA mutant in tomato (Solanum lycopersicum): effects on the seed and vegetative plant. J Exp Bot 59: 585-593

Pubmed: [Author and Title](#)

CrossRef: [Author and Title](#)

Google Scholar: [Author Only](#) [Title Only](#) [Author and Title](#)

Battaglia R, Colombo M, Kater MM (2009) The ins and outs of ovule development. In L. Ostergaard, Fruit Development and Seed Dispersal, Ann Plant Rev Vol 38. Wiley-Blackwell, Oxford, UK. pp 70-106. doi: 10.1002/9781444314557.ch3

Pubmed: [Author and Title](#)

CrossRef: [Author and Title](#)

Google Scholar: [Author Only](#) [Title Only](#) [Author and Title](#)

Beeckman T, De Rycke R, Viane R, Inze D (2000) Histological study of seed coat development in Arabidopsis thaliana. J Plant Res 113: 139-148

Pubmed: [Author and Title](#)

CrossRef: [Author and Title](#)

Google Scholar: [Author Only](#) [Title Only](#) [Author and Title](#)

Belda-Palazon B, Ruiz L, Marti E, Tarraga S, Tiburcio AF, Culiñez F, Farras R, Carrasco P, Ferrando A (2012) Aminopropyltransferases involved in polyamine biosynthesis localize preferentially in the nucleus of plant cells. PLoS One 7: e46907

Pubmed: [Author and Title](#)

CrossRef: [Author and Title](#)

Google Scholar: [Author Only](#) [Title Only](#) [Author and Title](#)

Bewley JD, Bradford KJ, Hilhorst HWM, Nonogaki H (2013). Seeds: Physiology of development, germination and dormancy. New York, NY: Springer. doi:10.1007/978-1-4614-4693-4

Pubmed: [Author and Title](#)

CrossRef: [Author and Title](#)

Google Scholar: [Author Only](#) [Title Only](#) [Author and Title](#)

Brambilla V, Kater M, Colombo L (2008) Ovule integument identity determination in Arabidopsis. Plant Sign Behav 3: e246-7

Pubmed: [Author and Title](#)

CrossRef: [Author and Title](#)

Google Scholar: [Author Only](#) [Title Only](#) [Author and Title](#)

Cao D, Hussain A, Cheng H, Peng J (2005) Loss of function of four DELLA genes leads to light- and gibberellin-independent seed germination in Arabidopsis. Planta 223: 105-113

Pubmed: [Author and Title](#)

CrossRef: [Author and Title](#)

Google Scholar: [Author Only](#) [Title Only](#) [Author and Title](#)

Cervantes E, Javier Martin J, Ardanuy R, de Diego JG, Tocino A (2010) Modeling the Arabidopsis seed shape by a cardioid: efficacy of the adjustment with a scale change with factor equal to the Golden Ratio and analysis of seed shape in ethylene mutants. J Plant Physiol 167: 408-410

Pubmed: [Author and Title](#)

CrossRef: [Author and Title](#)

Google Scholar: [Author Only](#) [Title Only](#) [Author and Title](#)

Cheng H, Qin L, Lee S, Fu X, Richards DE, Cao D, Luo D, Harberd NP, Peng J (2004) Gibberellin regulates Arabidopsis floral development via suppression of DELLA protein function. Development 131: 1055-1064

Pubmed: [Author and Title](#)

CrossRef: [Author and Title](#)

Google Scholar: [Author Only](#) [Title Only](#) [Author and Title](#)

Cox CM, Swain SM (2006) Localised and non-localised promotion of fruit development by seeds in Arabidopsis. Funct Plant Biol 33: 1-8

Pubmed: [Author and Title](#)

CrossRef: [Author and Title](#)

Google Scholar: [Author Only](#) [Title Only](#) [Author and Title](#)

de Lucas M, Daviere JM, Rodriguez-Falcon M, Pontin M, Iglesias-Pedraz JM, Lorrain S, Fankhauser C, Blazquez MA, Titarenko E, Prat S (2008) A molecular framework for light and gibberellin control of cell elongation. *Nature* 451: 480-484

Pubmed: [Author and Title](#)

CrossRef: [Author and Title](#)

Google Scholar: [Author Only](#) [Title Only](#) [Author and Title](#)

Daviere JM, Achard P (2016) A Pivotal Role of DELLAs in Regulating Multiple Hormone Signals. *Mol Plant* 9: 10-20

Pubmed: [Author and Title](#)

CrossRef: [Author and Title](#)

Google Scholar: [Author Only](#) [Title Only](#) [Author and Title](#)

Dill A, Jung HS, Sun T-p (2001) The DELLA motif is essential for gibberellin-induced degradation of RGA. *Proc Natl Acad Sci USA* 98: 14162-14167

Pubmed: [Author and Title](#)

CrossRef: [Author and Title](#)

Google Scholar: [Author Only](#) [Title Only](#) [Author and Title](#)

Dorcey E, Urbez C, Blazquez MA, Carbonell J, Perez-Amador MA (2009) Fertilization-dependent auxin response in ovules triggers fruit development through the modulation of gibberellin metabolism in *Arabidopsis*. *Plant J* 58: 318-332

Pubmed: [Author and Title](#)

CrossRef: [Author and Title](#)

Google Scholar: [Author Only](#) [Title Only](#) [Author and Title](#)

Eshed Y, Baum SF, Perea JV, Bowman JL (2001) Establishment of polarity in lateral organs of plants. *Curr Biol* 11: 1251-1260

Pubmed: [Author and Title](#)

CrossRef: [Author and Title](#)

Google Scholar: [Author Only](#) [Title Only](#) [Author and Title](#)

Feng S, Martinez C, Gusmaroli G, Wang Y, Zhou J, Wang F, Chen L, Yu L, Iglesias-Pedraz JM, Kircher S, Schäfer E, Fu X, Fan L-M, Deng XW (2008) Coordinated regulation of *Arabidopsis thaliana* development by light and gibberellins. *Nature* 451: 475-479

Pubmed: [Author and Title](#)

CrossRef: [Author and Title](#)

Google Scholar: [Author Only](#) [Title Only](#) [Author and Title](#)

Ferrando A, Koncz-Kalman Z, Farras R, Tiburcio A, Schell J, Koncz C (2001) Detection of in vivo protein interactions between Snf1-related kinase subunits with intron-tagged epitope-labelling in plants cells. *Nucleic Acids Res* 29: 3685-3693

Pubmed: [Author and Title](#)

CrossRef: [Author and Title](#)

Google Scholar: [Author Only](#) [Title Only](#) [Author and Title](#)

Franco-Zorrilla JM, Lopez-Vidriero I, Carrasco JL, Godoy M, Vera P, Solano R (2014) DNA-binding specificities of plant transcription factors and their potential to define target genes. *Proc Natl Acad Sci USA* 111: 2367-2372

Pubmed: [Author and Title](#)

CrossRef: [Author and Title](#)

Google Scholar: [Author Only](#) [Title Only](#) [Author and Title](#)

Fuentes S, Ljung K, Sorefan K, Alvey E, Harberd NP, Ostergaard L (2012) Fruit growth in *Arabidopsis* occurs via DELLA-dependent and DELLA-independent gibberellin responses. *Plant Cell* 24: 3982-3996

Pubmed: [Author and Title](#)

CrossRef: [Author and Title](#)

Google Scholar: [Author Only](#) [Title Only](#) [Author and Title](#)

Gallego-Giraldo C, Hu J, Urbez C, Gomez MD, Sun T-p, Perez-Amador MA (2014) Role of the gibberellin receptors GID1 during fruit-set in *Arabidopsis*. *Plant J* 79: 1020-1032

Pubmed: [Author and Title](#)

CrossRef: [Author and Title](#)

Google Scholar: [Author Only](#) [Title Only](#) [Author and Title](#)

Galvao VC, Horrer D, Küttner F, Schmid M (2012) Spatial control of flowering by DELLA proteins in *Arabidopsis thaliana*. *Development* 139: 4072-4082

Pubmed: [Author and Title](#)

CrossRef: [Author and Title](#)

Google Scholar: [Author Only](#) [Title Only](#) [Author and Title](#)

Gomez MD, Beltran JP, Cañas L (2004) The pea END1 promoter drives anther-specific gene expression in different plant species. *Planta* 219: 967-981

Pubmed: [Author and Title](#)

CrossRef: [Author and Title](#)

Google Scholar: [Author Only](#) [Title Only](#) [Author and Title](#)

Gomez MD, Urbez C, Perez-Amador MA, Carbonell J (2011) Characterization of constricted fruit (ctf) mutant uncovers a role for AtMYB117/LOF1 in ovule and fruit development in *Arabidopsis thaliana*. *PLoS ONE* 6: e18760

Pubmed: [Author and Title](#)

CrossRef: [Author and Title](#)

Google Scholar: [Author Only](#) [Title Only](#) [Author and Title](#)

Gutierrez L, Van Wuytswinkel O, Castelain M, Bellini C (2007) Combined networks regulating seed maturation. *Trends Plant Sci* 12: 294-300

Pubmed: [Author and Title](#)

CrossRef: [Author and Title](#)

Google Scholar: [Author Only](#) [Title Only](#) [Author and Title](#)

Gupta R, Chakrabarty SK (2013) Gibberellic acid in plant: still a mystery unresolved. Plant Signal Behav 8: e25504

Pubmed: [Author and Title](#)

CrossRef: [Author and Title](#)

Google Scholar: [Author Only](#) [Title Only](#) [Author and Title](#)

Haughn G, Chaudhury A (2005) Genetic analysis of seed coat development in Arabidopsis. Trends Plant Sci 10: 472-477

Pubmed: [Author and Title](#)

CrossRef: [Author and Title](#)

Google Scholar: [Author Only](#) [Title Only](#) [Author and Title](#)

Hawker NP, Bowman JL (2004) Roles for Class III HD-Zip and KANADI genes in Arabidopsis root development. Plant Physiol 135: 2261-2270

Pubmed: [Author and Title](#)

CrossRef: [Author and Title](#)

Google Scholar: [Author Only](#) [Title Only](#) [Author and Title](#)

Holdsworth MJ, Bentsink L, Soppe WJJ (2008) Molecular networks regulating Arabidopsis seed maturation, after-ripening, dormancy and germination. New Phytol 179: 33-54

Pubmed: [Author and Title](#)

CrossRef: [Author and Title](#)

Google Scholar: [Author Only](#) [Title Only](#) [Author and Title](#)

Hu J, Mitchum MG, Barnaby N, Ayele BT, Ogawa M, Nam E, Lai WC, Hanada A, Alonso JM, Ecker JR, Swain SM, Yamaguchi S, Kamiya Y, Sun T-p (2008) Potential sites of bioactive gibberellin production during reproductive growth in Arabidopsis. Plant Cell 20: 320-336

Pubmed: [Author and Title](#)

CrossRef: [Author and Title](#)

Google Scholar: [Author Only](#) [Title Only](#) [Author and Title](#)

Ikeda A, Ueguchi-Tanaka M, Sonoda Y, Kitano H, Koshioka M, Futsuhara Y, Matsuoka M, Yamaguchi J (2001) slender rice, a constitutive gibberellin response mutant, is caused by a null mutation of the SLR1 gene, an ortholog of the height-regulating gene GAI/RGARHT/D8. Plant Cell 13: 999-1010

Pubmed: [Author and Title](#)

CrossRef: [Author and Title](#)

Google Scholar: [Author Only](#) [Title Only](#) [Author and Title](#)

Jasinski S, Tattersall A, Piazza P, Hay A, Martinez-Garcia JF, Schmitz G, Theres K, McCormick S, Tsiantis M (2008) PROCERA encodes a DELLA protein that mediates control of dissected leaf form in tomato. Plant J 56: 603-612

Pubmed: [Author and Title](#)

CrossRef: [Author and Title](#)

Google Scholar: [Author Only](#) [Title Only](#) [Author and Title](#)

Kelley DR, Gasser CS (2009) Ovule development: genetic trends and evolutionary considerations. Sex Plant Reprod 22: 229-234

Pubmed: [Author and Title](#)

CrossRef: [Author and Title](#)

Google Scholar: [Author Only](#) [Title Only](#) [Author and Title](#)

Kelley DR, Skinner DJ, Gasser CS (2009) Roles of polarity determinants in ovule development. Plant J 57: 1054-1064

Pubmed: [Author and Title](#)

CrossRef: [Author and Title](#)

Google Scholar: [Author Only](#) [Title Only](#) [Author and Title](#)

Kelley DR, Arreola A, Gallagher TL, Gasser CS (2012) ETTIN (ARF3) physically interacts with KANADI proteins to form a functional complex essential for integument development and polarity determination in Arabidopsis. Development 139: 1105-1109

Pubmed: [Author and Title](#)

CrossRef: [Author and Title](#)

Google Scholar: [Author Only](#) [Title Only](#) [Author and Title](#)

Kim DH, Yamaguchi S, Lim S, Oh E, Park J, A Hanada A, Kamiya Y, Choi G (2008) SOMNUS, a CCCH-type zinc finger protein in Arabidopsis, negatively regulates light-dependent seed germination downstream of PIL5. Plant Cell 20: 1260-1277

Pubmed: [Author and Title](#)

CrossRef: [Author and Title](#)

Google Scholar: [Author Only](#) [Title Only](#) [Author and Title](#)

Lim S, Park J, Lee N, Jeong J, Toh S, Watanabe A, Kim J, Kang H, Kim DH, Kawakami N, Choi G (2013) ABA-insensitive3, ABA-insensitive5, and DELLAs interact to activate the expression of SOMNUS and other high-temperature-inducible genes in imbibed seeds in Arabidopsis. Plant Cell 25: 4863-4878

Pubmed: [Author and Title](#)

CrossRef: [Author and Title](#)

Google Scholar: [Author Only](#) [Title Only](#) [Author and Title](#)

Lee S, Cheng H, King KE, Wang W, He Y, Hussain A, Lo J, Harberd NP, Peng J (2002) Gibberellin regulates Arabidopsis seed germination via RGL2, a GAI/RGA-like gene whose expression is up-regulated following imbibition. Genes Dev 16: 646-658

Pubmed: [Author and Title](#)

CrossRef: [Author and Title](#)

Google Scholar: [Author Only](#) [Title Only](#) [Author and Title](#)

Leon-Kloosterziel KM, Keijzer CJ, Koornneef M (1994) A Seed Shape Mutant of Arabidopsis That Is Affected in Integument Development. Plant Cell 6: 385-392

Pubmed: [Author and Title](#)

Downloaded from www.plantphysiol.org on October 31, 2016 - Published by www.plantphysiol.org
Copyright © 2016 American Society of Plant Biologists. All rights reserved.

CrossRef: [Author and Title](#)
Google Scholar: [Author Only Title Only Author and Title](#)

Marin-de la Rosa N, Sotillo B, Miskolczi P, Gibbs DJ, Vicente J, Carbonero P, Onate-Sanchez L, Holdsworth MJ, Bhalerao R, Alabadi D, Blazquez MA (2014) Large-scale identification of gibberellin-related transcription factors defines group VII ERFs as functional DELLA partners. *Plant Physiol* 166: 1022-1032

Pubmed: [Author and Title](#)
CrossRef: [Author and Title](#)
Google Scholar: [Author Only Title Only Author and Title](#)

Marin-de la Rosa N, Pfeiffer A, Hill K, Locascio A, Bhalerao RP, Miskolczi P, Grønlund AL, Wanchoo-Kohli A, Thomas SG, Bennett MJ, Lohmann JU, Blazquez MA, Alabadi D (2015) Genome wide binding site analysis reveals transcriptional coactivation of cytokinin-responsive genes by DELLA proteins. *PLoS Genet* 11: e1005337

Pubmed: [Author and Title](#)
CrossRef: [Author and Title](#)
Google Scholar: [Author Only Title Only Author and Title](#)

McAbee JM, Hill TA, Skinner DJ, Izhaki A, Hauser BA, Meister RJ, Venugopala Reddy G, Meyerowitz EM, Bowman JL, Gasser CS (2006) ABERRANT TESTASHAPE encodes a KANADI family member, linking polarity determination to separation and growth of Arabidopsis ovule integuments. *Plant J* 46: 522-531

Pubmed: [Author and Title](#)
CrossRef: [Author and Title](#)
Google Scholar: [Author Only Title Only Author and Title](#)

Meister RJ, Kotow LM, Gasser CS (2002) SUPERMAN attenuates positive INNER NO OUTER autoregulation to maintain polar development of Arabidopsis ovule outer integuments. *Development* 129: 4281-4289

Pubmed: [Author and Title](#)
CrossRef: [Author and Title](#)
Google Scholar: [Author Only Title Only Author and Title](#)

Mitchum MG, Yamaguchi S, Hanada A, Kuwahara A, Yoshioka Y, Kato T, Tabata S, Kamiya Y, Sun T-p (2006) Distinct and overlapping roles of two gibberellin 3-oxidases in Arabidopsis development. *Plant J* 45: 804-818

Pubmed: [Author and Title](#)
CrossRef: [Author and Title](#)
Google Scholar: [Author Only Title Only Author and Title](#)

Modrusan Z, Reiser L, Feldmann KA, Fischer RL, Haughn GW (1994) Homeotic transformation of ovules into carpel-like structures in Arabidopsis. *Plant Cell* 6: 333-349

Pubmed: [Author and Title](#)
CrossRef: [Author and Title](#)
Google Scholar: [Author Only Title Only Author and Title](#)

Moubaydin L, Perilli S, Dello Iorio R, Di Mambro R, Costantino P, Sabatini S (2010) The rate of cell differentiation controls the Arabidopsis root meristem growth phase. *Curr Biol* 20: 1138-1143

Pubmed: [Author and Title](#)
CrossRef: [Author and Title](#)
Google Scholar: [Author Only Title Only Author and Title](#)

Murashige T, Skoog F (1962) A revised medium for rapid growth and bioassays with tobacco tissue culture. *Physiol Plant* 15: 437-497

Pubmed: [Author and Title](#)
CrossRef: [Author and Title](#)
Google Scholar: [Author Only Title Only Author and Title](#)

Nonogaki H (2014) Seed dormancy and germination - emerging mechanisms and new hypotheses. *Front Plant Sci* 5: 233

Pubmed: [Author and Title](#)
CrossRef: [Author and Title](#)
Google Scholar: [Author Only Title Only Author and Title](#)

Park J, Lee N, Kim W, Lim S, Choi G (2011) ABI3 and PIL5 collaboratively activate the expression of SOMNUS by directly binding to its promoter in imbibed Arabidopsis seeds. *Plant Cell* 23: 1404-1415

Pubmed: [Author and Title](#)
CrossRef: [Author and Title](#)
Google Scholar: [Author Only Title Only Author and Title](#)

Peng J, Carol P, Richards DE, King KE, Cowling RJ, Murphy GP, Harberd NP (1997) The Arabidopsis GAI gene defines a signaling pathway that negatively regulates gibberellin responses. *Genes Dev* 11: 3194-3205

Pubmed: [Author and Title](#)
CrossRef: [Author and Title](#)
Google Scholar: [Author Only Title Only Author and Title](#)

Porri A, Torti S, Romera-Branchat M, Coupland G (2012) Spatially distinct regulatory roles for gibberellins in the promotion of flowering of Arabidopsis under long photoperiods. *Development* 139: 2198-2209

Pubmed: [Author and Title](#)
CrossRef: [Author and Title](#)
Google Scholar: [Author Only Title Only Author and Title](#)

Prasad K, Zhang X, Tobon E, Ambrose BA (2010) The Arabidopsis B-sister MADS-box protein, GORDITA, represses fruit growth and contributes to integument development. *Plant J* 62: 203-214

Pubmed: [Author and Title](#)

CrossRef: [Author and Title](#)
Google Scholar: [Author Only Title Only Author and Title](#)

Ray A, Robinson-Beers K, Ray S, Baker S C, Lang JD, Preuss D, Milligan SB, Gasser CS (1994) Arabidopsis floral homeotic gene BELL (BEL1) controls ovule development through negative regulation of AGAMOUS gene (AG). Proc Natl Acad Sci USA 91: 5761-5765

Pubmed: [Author and Title](#)
CrossRef: [Author and Title](#)
Google Scholar: [Author Only Title Only Author and Title](#)

Reiser L, Modrusan Z, Margossian L, Samach A, Ohad N, Haughn GW, Fischer RL (1995) The BELL1 gene encodes a homeodomain protein involved in pattern formation in the Arabidopsis ovule primordium. Cell 83: 735-742

Pubmed: [Author and Title](#)
CrossRef: [Author and Title](#)
Google Scholar: [Author Only Title Only Author and Title](#)

Riechmann JL, Heard J, Martin G, Reuber L, Jiang C, Keddie J, Adam L, Pineda O, Ratcliffe OJ, Samaha RR, Creelman R, Pilgrim M, Broun P, Zhang JZ, Ghandehari D, Sherman BK, Yu G (2000) Arabidopsis transcription factors: genome-wide comparative analysis among eukaryotes. Science 290: 2105-2110

Pubmed: [Author and Title](#)
CrossRef: [Author and Title](#)
Google Scholar: [Author Only Title Only Author and Title](#)

Rieu I, Ruiz-Rivero O, Fernandez-Garcia N, Griffiths J, Powers SJ, Gong F, Linhartova T, Eriksson S, Nilsson O, Thomas SG, Phillips AL, Hedden P (2008) The gibberellin biosynthetic genes AtGA20ox1 and AtGA20ox2 act, partially redundantly, to promote growth and development throughout the Arabidopsis life cycle. Plant J 53: 488-504

Pubmed: [Author and Title](#)
CrossRef: [Author and Title](#)
Google Scholar: [Author Only Title Only Author and Title](#)

Sakai H, Aoyama T, Bono H, Oka A (1998) Two component response regulators from Arabidopsis thaliana contain a putative DNA-binding motif. Plant Cell Physiol 39: 1232-1239

Pubmed: [Author and Title](#)
CrossRef: [Author and Title](#)
Google Scholar: [Author Only Title Only Author and Title](#)

Seo M, Jikumaru Y, Kamiya Y (2011) Profiling of hormones and related metabolites in seed dormancy and germination studies. Methods Mol Biol 773: 99-111

Pubmed: [Author and Title](#)
CrossRef: [Author and Title](#)
Google Scholar: [Author Only Title Only Author and Title](#)

Sieber P, Gheyselinck J, Gross-Hardt R, Laux T, Grossniklaus U, Schneitz K (2004) Pattern formation during early ovule development in Arabidopsis thaliana. Dev Biol 273: 321-334

Pubmed: [Author and Title](#)
CrossRef: [Author and Title](#)
Google Scholar: [Author Only Title Only Author and Title](#)

Silverstone AL, Jun, HS, Dill A, Kawaide H, Kamiya Y, Sun T-p (2001) Repressing a repressor: gibberellin-induced rapid reduction of the RGA protein in Arabidopsis. Plant Cell 13: 1555-1566

Pubmed: [Author and Title](#)
CrossRef: [Author and Title](#)
Google Scholar: [Author Only Title Only Author and Title](#)

Schneitz K, Huiskamp M, Pruitt RE (1995) Wild-type ovule development in Arabidopsis thaliana: a light microscope study of cleared whole-mount tissue. Plant J 7: 731-749

Pubmed: [Author and Title](#)
CrossRef: [Author and Title](#)
Google Scholar: [Author Only Title Only Author and Title](#)

Smyth DR, Bowman JL, Meyerowitz EM (1990) Early flower development in Arabidopsis. Plant Cell 2: 755-767

Pubmed: [Author and Title](#)
CrossRef: [Author and Title](#)
Google Scholar: [Author Only Title Only Author and Title](#)

Sun T-p (2011) The molecular mechanism and evolution of the GA-GID-DELLA signaling module in plants. Curr Biol 21: 338-345

Pubmed: [Author and Title](#)
CrossRef: [Author and Title](#)
Google Scholar: [Author Only Title Only Author and Title](#)

Sun T-p (2010) Gibberellin-GID1-DELLA: a pivotal regulatory module for plant growth and development. Plant Physiol 154: 567-570

Pubmed: [Author and Title](#)
CrossRef: [Author and Title](#)
Google Scholar: [Author Only Title Only Author and Title](#)

Talon M, Koornneef M, Zeevaart JA (1990) Endogenous gibberellins in Arabidopsis thaliana and possible steps blocked in the biosynthetic pathways of the semidwarf ga4 and ga5 mutants. Proc Natl Acad Sci USA 87: 7983-7987

Pubmed: [Author and Title](#)
CrossRef: [Author and Title](#)
Google Scholar: [Author Only Title Only Author and Title](#)

Truernit E, Bauby H, Dubreucq B, Grandjean O, Runions J, Barthelemy J, Palauqui JC (2008) High-resolution whole-mount imaging of three-dimensional tissue organization and gene expression enables the study of Phloem development and structure in *Arabidopsis*. *Plant Cell* 20:1494-1503

Pubmed: [Author and Title](#)

CrossRef: [Author and Title](#)

Google Scholar: [Author Only](#) [Title Only](#) [Author and Title](#)

Vera-Sirera F, Gomez MD, Perez-Amador MA (2015) DELLA proteins, a group of GRAS transcription regulators, mediate gibberellin signaling. In DH Gonzalez, *Plant Transcription Factors: Evolutionary, Structural and Functional Aspects*. Ed. Elsevier/Academic Press, San Diego, pp 313-328

Pubmed: [Author and Title](#)

CrossRef: [Author and Title](#)

Google Scholar: [Author Only](#) [Title Only](#) [Author and Title](#)

Villanueva JM, Broadhvest J, Hauser BA, Meister RJ, Schneitz K, Gasser CS (1999) INNER NO OUTER regulates abaxial- adaxial patterning in *Arabidopsis* ovules. *Genes Develop* 13: 3160-3169

Pubmed: [Author and Title](#)

CrossRef: [Author and Title](#)

Google Scholar: [Author Only](#) [Title Only](#) [Author and Title](#)

Vivian-Smith A, Koltunow AM (1999) Genetic analysis of growth-regulator-induced parthenocarp in *Arabidopsis*. *Plant Physiol* 121: 437-451

Pubmed: [Author and Title](#)

CrossRef: [Author and Title](#)

Google Scholar: [Author Only](#) [Title Only](#) [Author and Title](#)

Vivian-Smith A, Luo M, Chaudhury A, Koltunow A (2001) Fruit development is actively restricted in the absence of fertilization in *Arabidopsis*. *Development* 128: 2321-2331

Pubmed: [Author and Title](#)

CrossRef: [Author and Title](#)

Google Scholar: [Author Only](#) [Title Only](#) [Author and Title](#)

Weigel D, Glazebrook J (2002) *Arabidopsis: A laboratory Manual*. Cold Spring Harbor Laboratory Press, Cold Spring Harbor, New York

Pubmed: [Author and Title](#)

CrossRef: [Author and Title](#)

Google Scholar: [Author Only](#) [Title Only](#) [Author and Title](#)

Weitbrecht K, Muller K, Leubner-Metzger G (2011) First off the mark: early seed germination. *J Exp Bot* 62: 3289-3309

Pubmed: [Author and Title](#)

CrossRef: [Author and Title](#)

Google Scholar: [Author Only](#) [Title Only](#) [Author and Title](#)

Western TL, Burn J, Tan WL, Skinner DJ, Martin-McCaffrey L, Moffatt BA, Haughn GW (2001) Isolation and characterization of mutants defective in seed coat mucilage secretory cell development in *Arabidopsis*. *Plant Physiol* 127: 998-1011

Pubmed: [Author and Title](#)

CrossRef: [Author and Title](#)

Google Scholar: [Author Only](#) [Title Only](#) [Author and Title](#)

Western TL, Haughn GW (1999) BELL1 and AGAMOUS genes promote ovule identity in *Arabidopsis thaliana*. *Plant J* 18: 329-336

Pubmed: [Author and Title](#)

CrossRef: [Author and Title](#)

Google Scholar: [Author Only](#) [Title Only](#) [Author and Title](#)

Wiesen LB, Bender RL, Paradis T, Larson A, Perera MADN, Nikolau BJ, Olszewski NE, Carter CJ (2016) A role for GIBBERELLIN 2-OXIDASE6 and gibberellins in regulating nectar production. *Mol Plant* doi: 10.1016/j.molp.2015.12.019

Pubmed: [Author and Title](#)

CrossRef: [Author and Title](#)

Google Scholar: [Author Only](#) [Title Only](#) [Author and Title](#)